Journal of Glaciology

Article

Cite this article: Mishra A, Nainwal HC, Bolch T, Shah SS, Shankar R (2022). Glacier inventory and glacier changes (1994–2020) in the Upper Alaknanda Basin, Central Himalaya. *Journal of Glaciology* 1–16. https://doi.org/10.1017/jog.2022.87

Received: 23 September 2020
Revised: 8 September 2022
Accepted: 9 September 2022

Key words:
Central Himalaya; climate change; debris-covered glaciers; glacier changes; glacier inventory

Author for correspondence:
Aditya Mishra,
E-mail: mishraaditya557@gmail.com

cambridge.org/jog

Glacier inventory and glacier changes (1994–2020) in the Upper Alaknanda Basin, Central Himalaya

Aditya Mishra[1], H. C. Nainwal[1], Tobias Bolch[2,3], Sunil Singh Shah[1] and R. Shankar[4]

[1]Department of Geology, H.N.B. Garhwal University, Srinagar Garhwal, Uttarakhand, India; [2]Department of Geography, University of Zurich, Zurich, Switzerland; [3]School of Geography & Sustainable Development, University of St. Andrews, Scotland, UK and [4]Institute of Mathematical Sciences, Chennai, Tamil Nadu, India

Abstract

Himalayan glaciers have been shrinking and losing mass rapidly since 1970s with an enhanced rate after 2000. The shrinkage is, however, quite heterogeneous and it is important to document individual glacier characteristics and their changes at the basin scale. We present an updated glacier inventory of the Upper Alaknanda Basin (UAB), Central Himalaya for the year 2020 and report area, debris cover and length changes for the periods 1994–2006 and 2006–2020 based on remote-sensing data. We identified 198 glaciers, comprising an area of 354.6 ± 8.5 km^2, and classified them according to their size and morphology. The glaciers of the basin lost 4.2 ± 2.9% (0.16 ± 0.11% a^{-1}) of their frontal area (from 368.6 ± 9.2 to 353.0 ± 5.3 km^2) from 1994 to 2020. The average retreat rate was higher in the period 2006–2020 (13.3 ± 1.8 m a^{-1}) in comparison to 1994–2006 (9.3 ± 1.9 m a^{-1}). However, the area change rate was similar for the two periods (0.14 ± 0.27% a^{-1} for 1994–2006 and 0.16 ± 0.19% a^{-1} for 2006–2020). The debris-covered area has increased by 13.4 ± 4.4% from 1994 to 2020. A comparison with previous studies in UAB indicates consistent area loss of ~0.15% a^{-1} since the 1960s.

1. Introduction

Himalayan glaciers are shrinking and losing mass at rates comparable to the other regions of the globe (Bolch and others, 2012; Azam and others, 2018; Hock and others, 2019; Hugonnet and others, 2021). The ice loss has clearly increased after 2000 which can mainly be attributed to the current phase of accelerated atmospheric warming in the region (Sakai and Fujita, 2017; Bolch and others, 2019; King and others, 2019; Maurer and others, 2019; Bhattacharya and others, 2021). Recent projections indicate that, depending on the climate scenario, Himalayan glaciers will lose between 30 and 60% of their current mass by the end of the 21st century (Kraaijenbrink and others, 2017; Rounce and others, 2020). This will adversely affect the run-off in the major river systems of High Mountain Asia (Bolch, 2017; Immerzeel and others, 2020; Azam and others, 2021), particularly during periods and years with low precipitation (Pritchard, 2019).

Remote-sensing and field-based measurements indicate that the glacier changes are variable throughout the Himalaya (Scherler and others, 2011; Kulkarni and Karyakarte, 2014; Azam and others, 2018). The general behaviour of the glaciers is driven by climate, primarily by temperature and precipitation (Oerlemans and others, 1998; Oerlemans, 2005). However, the individual glacier response to the climatic forcing is strongly controlled by non-climatic factors determined by topography and the extent of debris cover (Salerno and others, 2017; Bush and Bishop, 2018). Consequently, two neighbouring basins that experience a similar regional climate could respond quite differently to climate forcing due to differences in the topographic settings (Garg and others, 2017). It is therefore important to assess the influence of climatic and topographic parameters on the glacier changes at basin scale. In this paper, we concentrate on the Upper Alaknanda Basin (UAB) in the Central Himalaya where such investigations are limited and no detailed up to date glacier inventory and estimates of glacier area change exist. A basin scale glacier inventory is available for the year 2006 and area changes were estimated for the period between 1968 and 2006 (Bhambri and others, 2011*a*). The present study focuses on the period from 2006 onwards. The previous work done in the UAB is reviewed below.

Bhambri and others (2011*a*) generated a glacier inventory of 83 glaciers in the basin for the year 2006 and reported an area loss of 5.7 ± 2.7% (0.14 ± 0.06% a^{-1}) from 1968 to 2006. Surface elevation changes of glaciers of UAB have been recently reported from 2000 to 2014 (Bandyopadhyay and others, 2019) and for the period 2000–2017 by Remya and others (2020). Both studies indicate an almost similar mean surface lowering, 0.37 m a^{-1} (2000–2014) and 0.33 m a^{-1} (2000–2017). Based on simple models validated with limited field data, the ice volume of the basin has been estimated to be 26.4 km^3 for the year 2016 (Mishra and others, 2021).

There have been several studies of the larger glaciers in the basin. Field studies on Satopanth and Bhagirath Kharak glaciers by Nainwal and others (2007) report three phases of glaciation in the valley during late quaternary period. Nainwal and others (2008) have

https://doi.org/10.1017/jog.2022.87 Published online by Cambridge University Press

estimated the length and area changes for Satopanth glacier to be 22.8 m a^{-1} and 0.314 km^2 and for Bhagirath Kharak glacier to be 7.42 m a^{-1} and 0.13 km^2 between 1962 and 2005. Nainwal and others (2016) have extended this analysis to the period 1937–2013 and reported retreat rates to be 5.7 and 6.0 m a^{-1} for Satopanth and Bhagirath Kharak glaciers respectively, corresponding to the area loss of 0.27 and 0.17 km^2. Mishra and others (2018) conducted ground-penetrating radar measurements and found the average ice thickness in the snout and upper ablation regions to be 40 and 100 m, respectively. Shah and others (2019) have reported sub-debris ice melt variability (1.5–1.7 cm d^{-1}) during 2015–17 based on the glaciological method. A modelling study on Satopanth Glacier to quantify the avalanche contribution in glacier mass balance shows that ~90% of the total glacier mass gain (~1.8 m w.e. a^{-1}) is dominated by avalanches (Laha and others, 2017). Remya and others (2020) found significant mass loss (0.55 ± 0.06 m w.e. a^{-1}) of Satopanth glacier during 2000–2017 as compared to 0.09 ± 0.04 m w.e. a^{-1} 1962–2000. Moreover, Garg and others (2017) have reported the results of a remote-sensing study on changes of length (~5–30 m a^{-1}) and area (~2.2%) of four glaciers of the UAB, during 1994–2015. Shukla and Garg (2020) have further estimated the spatio-temporal changes in the surface ice velocities of these glaciers. The study shows consistent reduction of average surface ice velocity from 22.6 m a^{-1} (1993–94) to 17.3 m a^{-1} (2000–01) and further decrease to 11.5 m a^{-1}. These previous studies, however, do not assess the characteristics of the individual glaciers in the basin. Furthermore, no study in the UAB has investigated area changes after 2006 including all the glaciers in the basin.

The objective of this work is to extend the current knowledge about the UAB by (i) generating a glacier inventory for 2020 including topographic parameters, snow line altitude and debris cover extent, (ii) estimating changes in area, length and debris cover area during the period 1994–2020 and (iii) correlating glacier area changes with climate and glacier-specific characteristics. We do this to contribute to the understanding of the complex processes of the dynamics of the collection of glaciers in the UAB in a rapidly changing climate.

2. Study area

Our study area, the UAB is located in the Central Himalayan region in Uttarakhand, a northern Indian state (Fig. 1). It is located between the latitude and longitude of 30.5–31°N and 79.25–79.72°E respectively. The Alaknanda River originates from the ~13 km long and ~750 m wide Satopanth Glacier (snout ~3880 meter above sea level [m a.s.l.]). UAB is a part of the Alaknanda Basin classified by the Geological Survey of India (GSI) as a third-order basin (5O 132) of Ganga River. The Alaknanda Basin has ~400 glaciers with an area of ~1200 km^2 (Raina and Srivastava, 2008). It contains all glaciers that contribute to the Alaknanda River after confluence with the Dhauliganga River at Vishnuprayag (Fig. 1). The UAB contains all glaciers that contribute to the Alaknanda River before its confluence with the Dhauliganga. The river system of UAB has a general orientation in north-south direction and its river tributaries and sub-catchments mostly have an east-west trend. The basin covers an area of ~1500 km^2 and ranges from ~1450 m (Vishnuprayag) to 7756 m a.s.l. (Kamet). Chaukhamba (~7138 m a.s.l.) is the second highest peak in the basin and the source of several large glaciers such as Satopanth, Bhagirath Kharak on the eastern and the north-eastern slopes and the Gangotri group of glaciers on the western slopes (Fig. 1).

A significant fraction of the glacierised area of the basin is debris-covered. Bhambri and others (2011*a*) report ~25% of the glacierised area being debris-covered. Field measurements on the Satopanth glacier (Shah and others, 2019) indicate that while the debris thickness decreases with elevation, there is a large spatial variation. The debris is mainly composed of kyanite-sillimanite schist, gneisses and leucogranites which belong to the Pandukeshwar and Pindari Formations (Valdiya and others, 1999).

The Central Himalaya receives most of its precipitation from the Indian summer monsoon. However, contribution from the westerlies in the region is also significant (Bookhagen and Burbank, 2006; Thayyen and Gergan, 2010). There are no instrumental climatic records available in the UAB. The Indian Meteorological Department (IMD) operates a weather station at Joshimath (~1650 m a.s.l.) located a little south of the basin. Measurements recorded mean annual precipitation of ~1100 mm from the period 1959–2013 (Kumar and others, 2017). The ambient mean monthly temperature from June was 29°C and that in October was ~5°C.

The Climate Research Unit (CRU) TS 4.04 data for the study area shows mean monthly temperatures varying from ~−7°C in January to ~11°C in July during 1901–2019 (Fig. 1b). The long-term mean monthly precipitation data show that maximum precipitation in UAB occurs during summer from June to September. The highest precipitation is recorded in the month of July (~151 mm) and August (~148 mm) followed by September (~83 mm) and June (~73 mm) (Fig. 1b). The mean annual air temperature and precipitation of the UAB for the period 1901–2019 were 2.2°C and ~700 mm, respectively. The summer precipitation contributed ~75% to the total annual precipitation.

3. Methodology

3.1. Data

We used different multi-temporal remote-sensing data 1994–2020 for glacier mapping detailed in Table 1. Satellite images of the ablation period (i.e. September and October) with minimum seasonal snow and cloud cover were selected. The Sentinel-2A image of 8 October 2020 was used as a reference image as it had most suitable conditions and matched best with our field-based differential GPS (DGPS) mapping over the frontal parts of Satopanth and Bhagirath Kharak glaciers conducted 6–7 October 2020 (Fig. 2). Two further Sentinel-2A images (acquired 13 September 2020 and 18 October 2020) were also checked to discard snow patches and misclassified shadow zones. The satellite data from the different sensors were co-registered with the Sentinel-2A images as a master image using the projective transformation algorithm in ERDAS Imagine 2014 (cf. Bolch and others, 2010*a*; Frey and others, 2012). In total, 32 common control points, such as confluences of streams, intersections of streams and roads, 'crossed ridges', and prominent peaks and moraines were selected to assess the horizontal accuracy. We assumed that no changes in these features had occurred. The common points were distributed throughout the study area with the highest concentration around the glacierised regions. We could achieve a root mean square error (RMSE) less than the pixel size of the images, i.e. ~16 m for TM and ~13 m for ASTER scenes. While the ASTER image has a relatively higher RMSE value and limited study area coverage, we used it in our study to compare the results of the previous study in UAB by Bhambri and others (2011*a*). A short wave infrared (SWIR) band is needed for automated glacier mapping owing to the distinctive reflectance and absorption properties of snow and ice as compared to visible and near infrared (NIR) bands (Paul and others, 2015). The SWIR bands of ASTER (band-4) and Sentinel (band-12) images have lower spatial resolutions of 30 and 20 m respectively, and were therefore resampled in ERDAS

https://doi.org/10.1017/jog.2022.87 Published online by Cambridge University Press

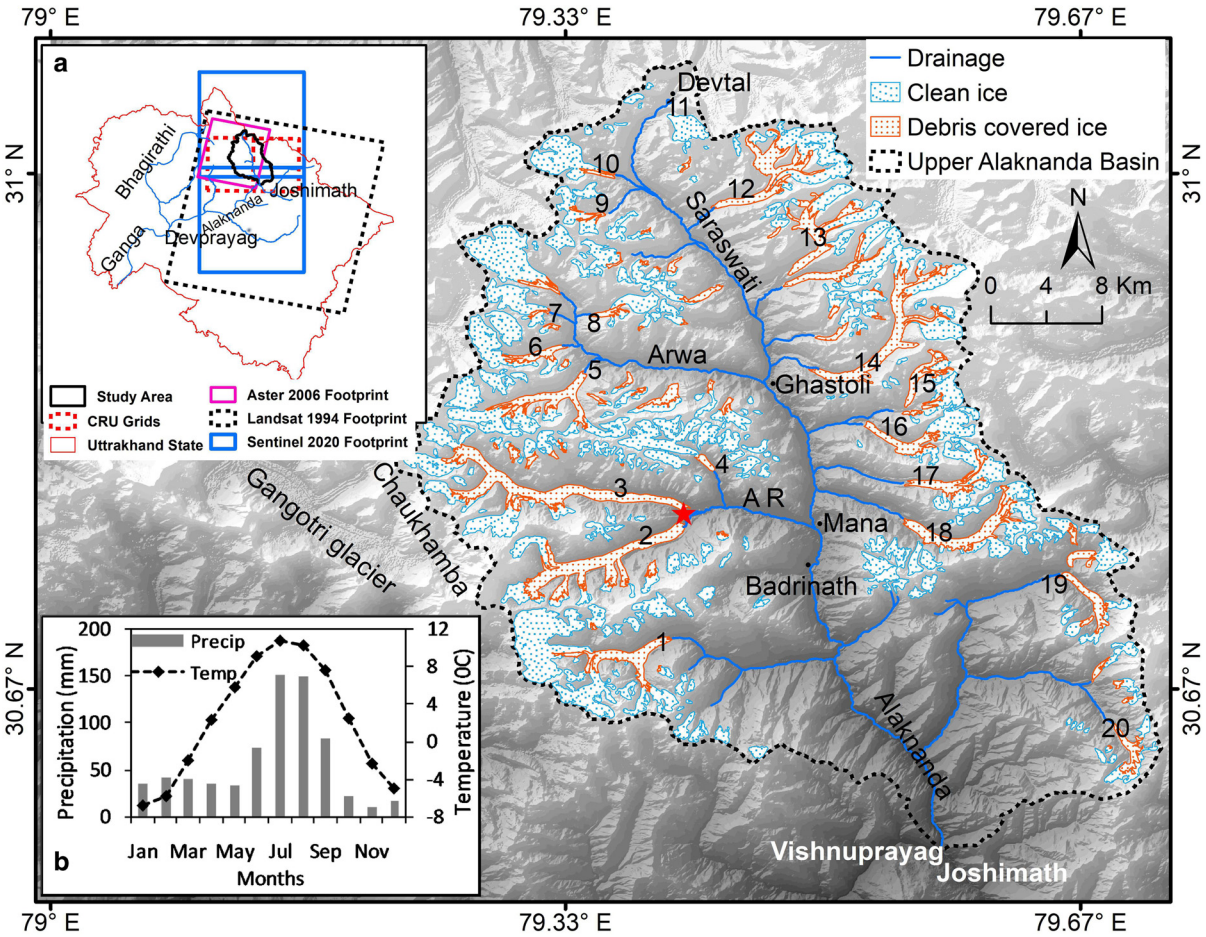

Fig. 1. Location map of the study area showing clean and debris-covered parts of the glaciers and main localities. Inset (a) Uttarakhand State and footprints of the satellite images used in the study, (b) climate diagram (1901–2019) for the basin extracted from CRU data. The numbers (1–20) indicate glaciers with length change estimations. The star shows the field surveyed snout locations of Satopanth (2) and Bhagirath Kharak (3) glaciers.

Imagine 2014 to 15 and 10 m, respectively, to match the resolution of the visible and NIR bands of the ASTER and Sentinel-2A images.

To extract the topographic information of the glaciers, the High Mountain Asia Digital Elevation Model (HMA DEM) (Shean, 2017) was used (Table 1). This DEM was in particular generated based on high-resolution WorldView images acquired during 2013 and 2016 and has a spatial resolution of 8 m.

We used the HMA DEM due to its better spatial resolution as compared to the SRTM DEM and ASTER GDEM for the best temporal fit to the Sentinel-2 data. The problem with HMA DEM is the occurrence of few data voids, especially in areas with very low correlation in the optical stereo imagery used, e.g. near steep slopes or cast shadows. To obtain full coverage, we interpolated these voids using nearest neighbour interpolation. Since the glacierised areas were free from data gaps and the purpose of the DEM was extract topographic parameters, the voids did not impact the results of our study.

Table 1. Details of the satellite data and digital elevation model (DEM) used in this study

Satellite/ sensor	Processing level	Date of acquisition	Spectral bands used	Spatial resolution (m)
Landsat 5 TM	L1TP	23 September 1994	Blue, green, red, NIR and SWIR	30
ASTER	L1T	9 October 2006	Green, red, NIR and SWIR	15 (30 m)
Sentinel 2A MSI	L1C	8 October 2020 13 September 2020 18 October 2020	Blue, green, red, NIR and SWIR	10 (20 m)
High Mountain Asia DEM		2013–2016	DEM	~8

TM, thematic mapper, NIR, near infrared; SWIR, shortwave infrared.

3.2. Glacier mapping

To map the glacier boundaries on the basis of satellite images, the recommendations of Global Land Ice Measurements from Space (GLIMS) initiative were followed (Paul and others, 2009, 2015; Racoviteanu and others, 2009). The extents of glaciers were manually delineated on-screen in ArcGIS 10.5 with an approximate scale of 1 : 10 000 using different band combinations, for example, NIR-Red-Green, SWIR-NIR-Red, Red-Blue-Green (Fig. 3). We preferred manual mapping as many of the glaciers in our study are debris-covered for which the automated methods fail or have a low accuracy due to similar spectral properties of the surrounding debris (Bhambri and others, 2011*a*; Frey and others, 2012).

The visual identification of the boundary of debris-covered glaciers is a challenging task particularly in the frontal regions (Bolch and others, 2010*a*; Paul and others, 2013). The boundaries in these regions were identified considering colour differences and the surrounding geomorphology, such as steep ice walls or

https://doi.org/10.1017/jog.2022.87 Published online by Cambridge University Press

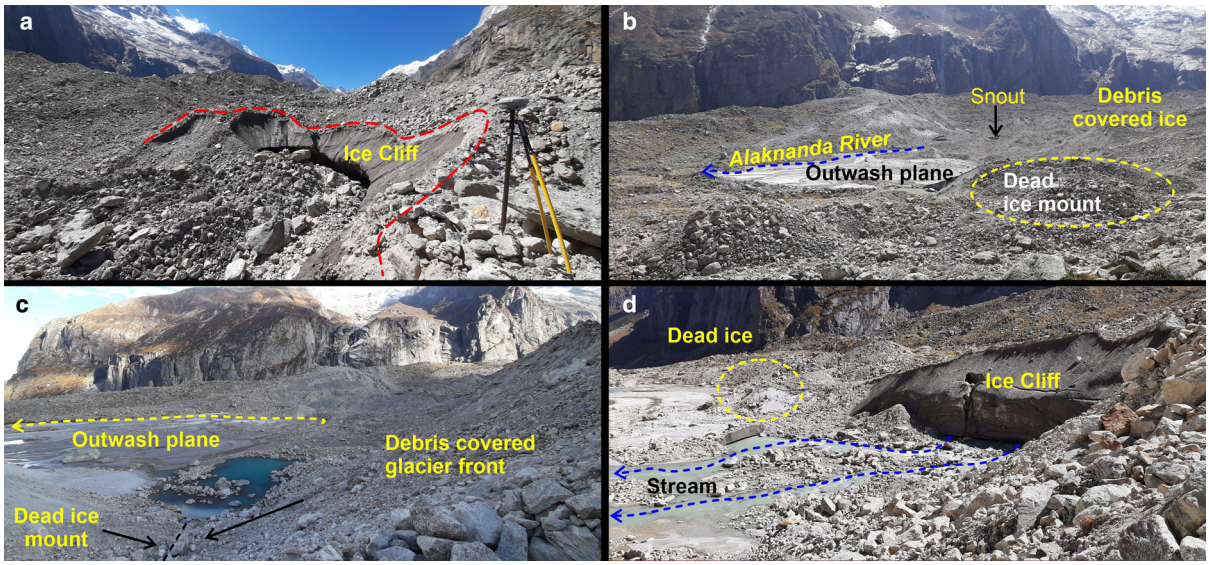

Fig. 2. Field photographs showing (a) the snout of Satopanth Glacier mapped with the help of DGPS on 7 October 2020, (b, c) the presence of dead ice mound, water pond and outwash plan in the vicinity of Satopanth Glacier, (d) the frontal part of Bhagirath Kharak Glacier (mapped on 6 October 2020) and associated dead ice (photos: A. Mishra 2020).

exposed ice faces, stream emerging points, outwash plains, lateral morainic ridges, water ponds and ice cliff shadows. The surface slope and shaded relief maps derived from the HMA DEM were used as additional information (Bolch and others, 2007; Bhambri and others, 2011*b*). The presence of dead ice mounds creates another difficulty in delineation of debris-covered glaciers because of their close vicinity to the glacier fronts. Hence, high-resolution (~0.5–2.5 m) images available in Google Earth were taken as additional information along with the presence of surface meltwater ponds which differ from supraglacial ponds by their different reflectance caused by different turbidity. Also, our field experience at Satopanth and Bhagirath Kharak glaciers (Fig. 2) helped us to delineate glacier boundaries especially near the glacier fronts.

The glacier inventory was prepared based on the 2020 Sentinel image with the smallest glacier area of a glacier being 0.02 km^2. A similar size threshold was used for the Himalayan glacier inventory by ICIMOD (Bajracharya and Shrestha, 2011) and, in Western Himalaya, by Frey and others (2012). The distinction between snow patches and small glaciers (<0.5 km^2) is crucial, since snow can accumulate for few years on mountain slopes and ridges. We excluded such seasonal snow patches by a visual interpretation of the additional Sentinel-2 images (Table 1) and high-resolution images of Google Earth along with field studies around Satopanth Glacier. For the glacier inventory, contiguous ice masses were separated into glaciers based on the HMA DEM, using hydrologic functions in ArcGIS and further checked and adjusted using shaded relief map and Google Earth 3-D views (Racoviteanu and others, 2009; Bolch and others, 2010*b*; Das and Sharma, 2018).

The late summer snowline altitude (SLA) was retrieved for the glacier inventory (2020) by manually delineating the snowline

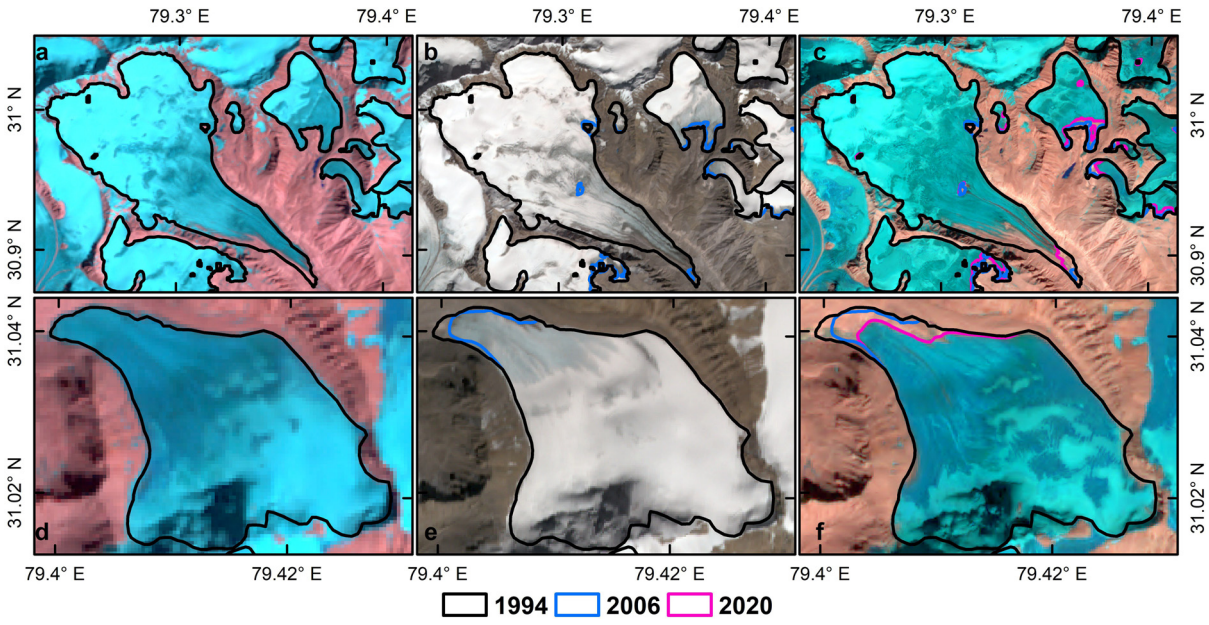

Fig. 3. Manually demarcated glacier outlines, (a, d) 1994 Landsat TM (1994), (b, e) ASTER (2006) and (c, f) Sentinel-2 (2020) images showing no visible changes in the upper regions of the glaciers.

https://doi.org/10.1017/jog.2022.87 Published online by Cambridge University Press

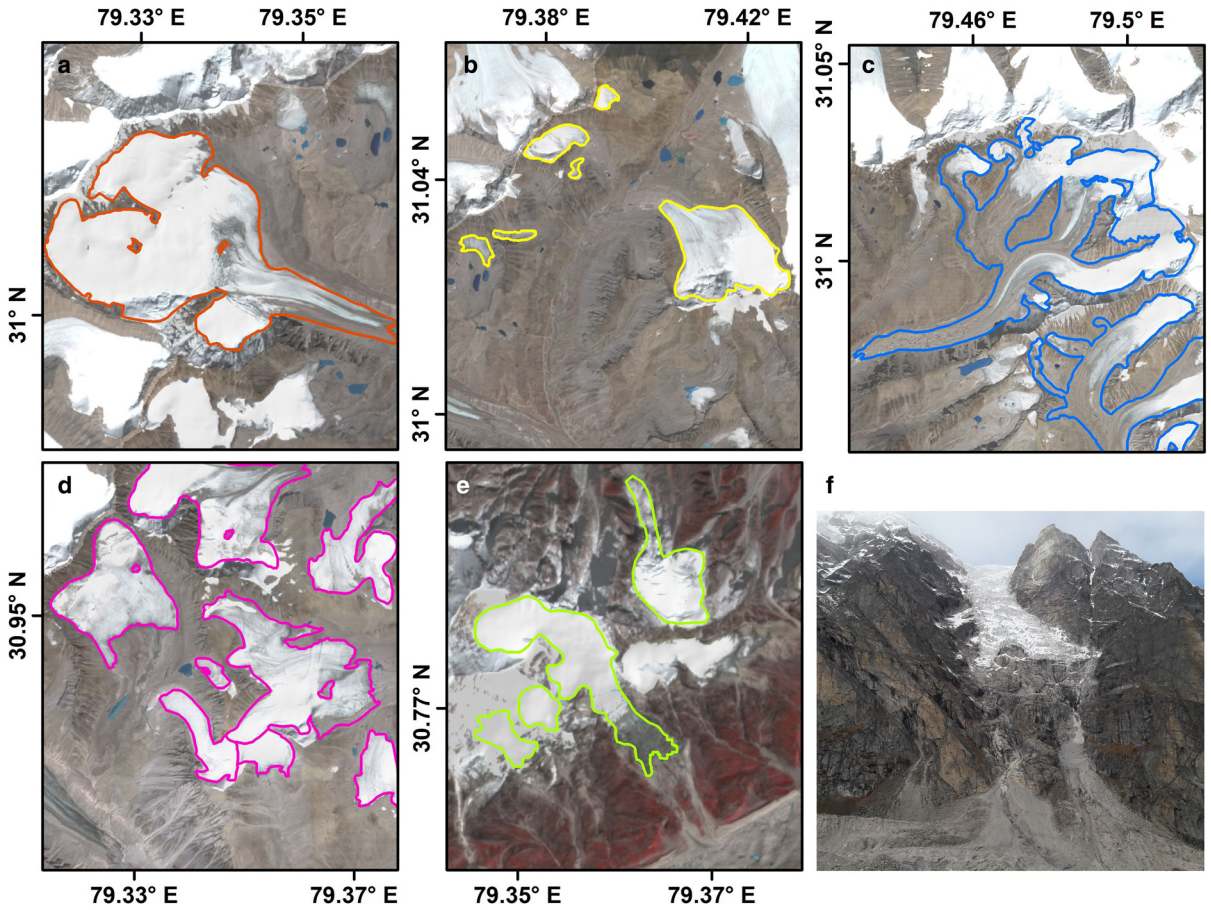

Fig. 4. Example of the morphological classification of glaciers of UAB mapped from Sentinel images (Hillshade map in the background): (a) simple basin, (b) cirque, (c) compound basin, (d) mountain glaciers, (e) hanging glacier, (f) field photograph of the hanging glacier (e) taken during fieldwork in 2016 (photo: A. Mishra 5 September 2016).

using the band combination SWIR (12)-NIR (8)-Green (3) of the master Sentinel-2 image (cf. Rabatel and others, 2005; Shukla and others, 2020). A buffer of 15 m was created on either side of the marked snowline and mean altitude of this buffer zone was extracted using the HMA DEM.

3.3. Quantification of glacier-specific characteristics

The mapped glaciers were classified based on their area and morphology. The coarse area ranges chosen were <0.5; 0.5–1; 1–5; 5–10; >10 km^2. The glaciers were categorised as valley and mountain glaciers, according to the GLIMS guidelines (Rau and others, 2005). Valley glaciers have well-defined accumulation and ablation areas and their form is controlled by the respective topography. Such glaciers follow pre-existing valley-shapes and are further divided into compound and simple basin. The remaining glaciers are those which lie on mountain slopes and terminate before reaching the main valley. Such glaciers are defined as cirque glaciers, hanging glaciers and mountain glaciers (Fig. 4).

The glacier outlines and the DEM enabled us to extract the elevation parameters of the glacier surface. Glacier area, perimeter, minimum, maximum and mean elevations, the elevation range and the mean slope of each glacier were extracted using zonal statistical tools in ArcGIS. Glacier lengths were calculated from manually drawn centre-lines. The aspect was calculated on the basis of the orientation of the centre-lines. In case of arc-shaped glaciers, the average direction of the trunk glacier was taken to determine the aspect.

3.4. Change detection analysis

Area changes of 138 glaciers were estimated for the periods 1994–2006 and 2006–2020. We could not map the area changes of all 198 glaciers of the 2020 inventory since not all of them were clearly visible in the Landsat image owing to partial cloud cover and limited coverage of the 2006 ASTER image. In total, 175 glaciers could be investigated for the period 1994–2020.

To calculate the glacier area-changes, the glacier-boundaries demarcated in the 'base image, 2020' were superimposed over the previous glacier-boundaries (cf. Bolch and others, 2010*a*, 2010*b*). The upper parts of the glacier showed no measurable changes during the study period (as also noted by Bhambri and others, 2011*a*), except around the internal rocks. Therefore, area changes were mainly in the vicinity of the fronts (Fig. 3). Several glaciers fragmented during the study period; in such cases, the total fragmented area was used to estimate the area change.

We calculated the length changes of selected UAB glaciers for both the periods (i.e. 1994–2006 and 2006–2020). The glaciers were selected on the basis of their frontal morphology: a well-defined glacier front and confined by lateral moraines and a straight and narrow glacier tongue. As most of the small glaciers (<5 km^2) in UAB have irregular fronts we discarded them and finally 20 larger glaciers (numbered 1–20 in Fig. 1) were chosen for length change measurements. The glacier-boundaries from the different years were superimposed over each other. For the estimation of glacier retreat, parallel lines were drawn on either side of the central flow-line (or along the maximum glacier length) at 50 m intervals (Supplementary Fig. S1); and the changes in length along each of these lines were then averaged (cf. Koblet and others, 2010; Bhambri and others, 2012).

https://doi.org/10.1017/jog.2022.87 Published online by Cambridge University Press

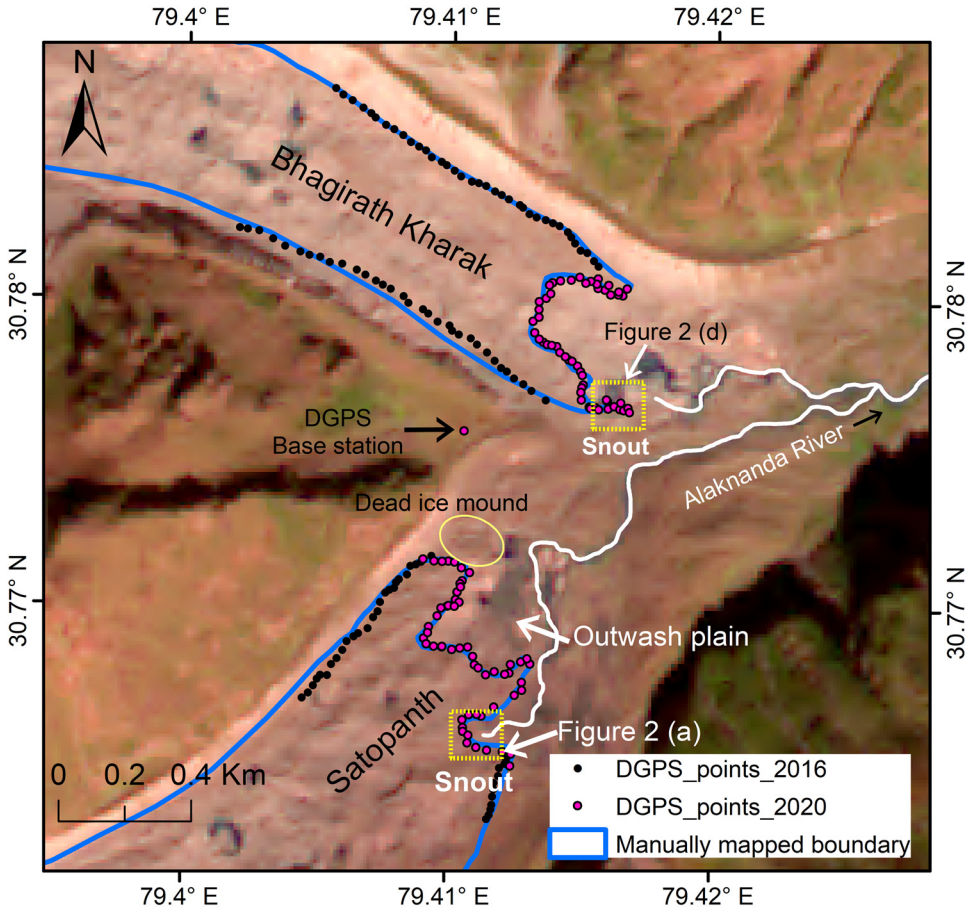

Fig. 5. Satopanth and Bhagirath Kharak glacier boundaries mapped by DGPS data in 2020 and manually demarcated glacier boundary (blue) based on the Sentinel-2 image (SWIR-NIR-Red) of the same year.

4. Uncertainty estimations

The uncertainties of the glacier boundaries were estimated in two ways: (a) by comparing the glacier outlines from the satellite image (2020) to a field survey done during the same period at Satopanth and Bhagirath Kharak glaciers, and (b) using the buffer method (Granshaw and Fountain, 2006; Bolch and others, 2010*a*; Chand and Sharma, 2015). The boundaries of Satopanth and Bhagirathi Kharak glacier fronts (Fig. 2) were mapped by a DGPS survey, having horizontal accuracy of ±10 cm. The difference between the surveyed DGPS points and the manually mapped boundaries over two glaciers was ~5 m at the front ice cliff regions and ~8–12 m at the debris-covered parts (Fig. 5).

To estimate the area uncertainties of all glaciers, the buffer method was used with buffer sizes of half of the pixel size or co-registration error between two images. These were 5, 6.5 and 8 m for the Sentinel-2, ASTER and Landsat TM images respectively. This resulted in an average mapping uncertainty of 3.5% for TM, 2.75% for ASTER and 2.3% for Sentinel-2. These estimates are consistent with the previously reported mapping uncertainties (Bolch and others, 2010*a*; Bhambri and others, 2011*a*; Paul and others, 2013; Chand and Sharma, 2015; Garg and others, 2017). The uncertainty in area changes was estimated according to the standard error propagation, as root sum square of the uncertainty for outlines mapped from different sources (Bhambri and others, 2011*a*).

The length uncertainty of the three satellite images of different years was estimated by considering the following equations (Hall and others, 2003):

$$\text{Uncertainty in retreat} = \sqrt{a^2 + b^2} + \sigma,$$

where '*a*' and '*b*' are spatial resolution of the images 1 and 2, respectively, and σ is the co-registration error which was 16 m in case of Landsat TM (1994) and 13 m for ASTER (2006). The resultant length change uncertainty was found to be 47.6 m TM and 31.0 m for ASTER.

5. Temperature and precipitation data

CRU data (version 4.04) (Harris and others, 2020) from 1901 to 2019 was used for the analysis of temperature and precipitation. The study area is located within two 0.5 degree grids (Fig. 1): grid 01 (30.75°N, 79.25°E) and grid 02 (30.75°N, 79.5°E). The trend was similar for these two grid points. Thus, we have averaged the two datasets. A statistical analysis shows that the averaging of both the grids does not affect the trend in the data (Supplementary Table S1). A non-parametric Mann–Kendall test was used to determine the statistical significance of the trend, and the magnitudes of the trend were obtained through a linear regression analysis (Bhambri and others, 2011*a*). The trend analysis has been done on annual basis.

6. Results

6.1. Glacier inventory

The 2020 inventory of the study area comprises 198 glaciers of different sizes, morphological types and extents of debris cover (Tables 2 and 3; Fig. 6). The total glacierised area is 354.6 ± 8.1 km^2, of which ~27% is covered with debris. Out of the 198 glaciers, 64 were debris-covered. While only 10 of the 198 glaciers have an area of more than 10 km^2, they occupy ~50% of the total

https://doi.org/10.1017/jog.2022.87 Published online by Cambridge University Press

Table 2. Glacier parameters of different area ranges

Parameters	Area range (km^2)					
	All	<0.5	0.5–1.0	1.0–5.0	5.0–10	>10
Number	198	106	35	41	6	10
Area (km^2)	354.6	21.6	22.9	84.5	46.2	179.4
% of area under debris cover	26.9	6.0	8.5	18.6	21.2	37.2
Mean elevation (m a.s.l.)	5269	5273	5201	5302	5445	5226
Median elevation (m a.s.l.)	5235	5310	5175	5280	5400	5125
Average snowline altitude (m a.s.l.)	5294	5262	5254	5338	5467	5352
Average elevation range (m)	611	345	628	911	1420	1677
Mean slope (°)	24	26	23	20	17	16

Table 3. Glacier parameters of different morphological types

Parameters	Cirque	Hanging glacier	Mountain glacier	Simple basin	Compound basin
Number of glaciers	27	47	82	31	11
Area (km^2)	13.3	23.6	50.6	89.6	177.5
% of area under debris cover	16.7	0.0	4.8	23.0	38.9
Mean elevation (m a.s.l.)	5300	5223	5282	5276	5165
Median elevation (m a.s.l.)	5285	5227	5273	5083	5006
Elevation range (m a.s.l.)	388	662	540	990	1866
Mean slope (°)	23	27	24	20	17
Average snowline altitude (m a.s.l.)	5257	5271	5312	5300	5323

glacierised area. The large glaciers tend to have compound basins; consequently about half the glacierised area is in compound basins. Of the morphological types the number of mountain glaciers is the highest (Fig. 7).

The area-elevation distribution shows that ~50% of the area is located at the elevation ~5200 m a.s.l. (Fig. 8a). However, the area of the large glaciers (>10 km^2) is much more broadly distributed in the elevation range 4700–5800 m a.s.l., consistent with debris-covered glaciers which tend to have long narrow tongues. The debris-covered area is broadly distributed between 3800 and 5850 m a.s.l. There are two prominent peaks of debris-covered extents at an elevation of 4350 and 5100 m a.s.l. This may be due to the location of snouts of large debris-covered glaciers at higher altitude. For example, the snout of Balabala Glacier (No-12 in Fig. 1) is located at an elevation of ~5040 m a.s.l. which is significantly higher than the glaciers (i.e. Bhagirath Kharak) having minimum elevations (~3880 m a.s.l.). The most frequent glacier aspect is north ($n = 41$), followed by south ($n = 39$), while glaciers facing southeast (65.2 ± 2.3 km^2) and southwest (63.2 ± 2.2 km^2) have the greatest area (Fig. 8b).

The snowline of the UAB glaciers is located at an elevation of ~5300 m a.s.l. with glaciers between 5 and 10 km^2 having the highest average snowline of 5467 m a.s.l. The SLA of large glaciers (>10 km^2) is located at a slightly lower elevation (5352 m a.s.l.) probably due to their large elevation range and low lying tongues. The glaciers <0.5 km^2 and of 0.5–1.0 km^2 in size have the SLA at a similar elevation of 5262 and 5254 m a.s.l., respectively. The hanging glaciers have a relatively higher mean slope (27°) than the mountain glaciers (24°). The mean slope is 24° which varies from 16° to 26° in >10 and <0.5 km^2 glacier sizes, respectively.

The extent of debris cover increases with the increasing size of the glacier. Large glaciers (>10 km^2) have ~35% of their area covered with debris; whereas the smaller glaciers (<0.5 km^2) are almost debris-free. In fact only 65 of the 198 glaciers had debris cover in 2020. Most of the debris-free glaciers are of <1 km^2 in size (Fig. 8c).

6.2. Area changes

The glacierised area of the basin has reduced from 368.6 ± 9.2 km^2 in 1994 to 353.0 ± 5.3 km^2 in 2020, a change of 4.2 ± 2.9% (0.16 ± 0.11% a^{-1}) (Table 4). The area loss of individual glaciers varied from 0.5 ± 0.8 to 38 ± 3.9% between 1994 and 2020. The relative area loss (%) has been grouped in six classes (<5; 5–10; 10–15; 15–20; 20–25 and >25) and geographical distribution (Fig. 9). The number of glaciers increased from 175 to 198 during the period of study due to fragmentation. The relative % area loss of small glaciers (<5 km^2) was ~8.5%, which was significantly larger than that of the large (>5 km^2) glaciers (~1.8%) from 1994 to 2020. Very small glaciers (<0.5 km^2) lost ~15% of their area.

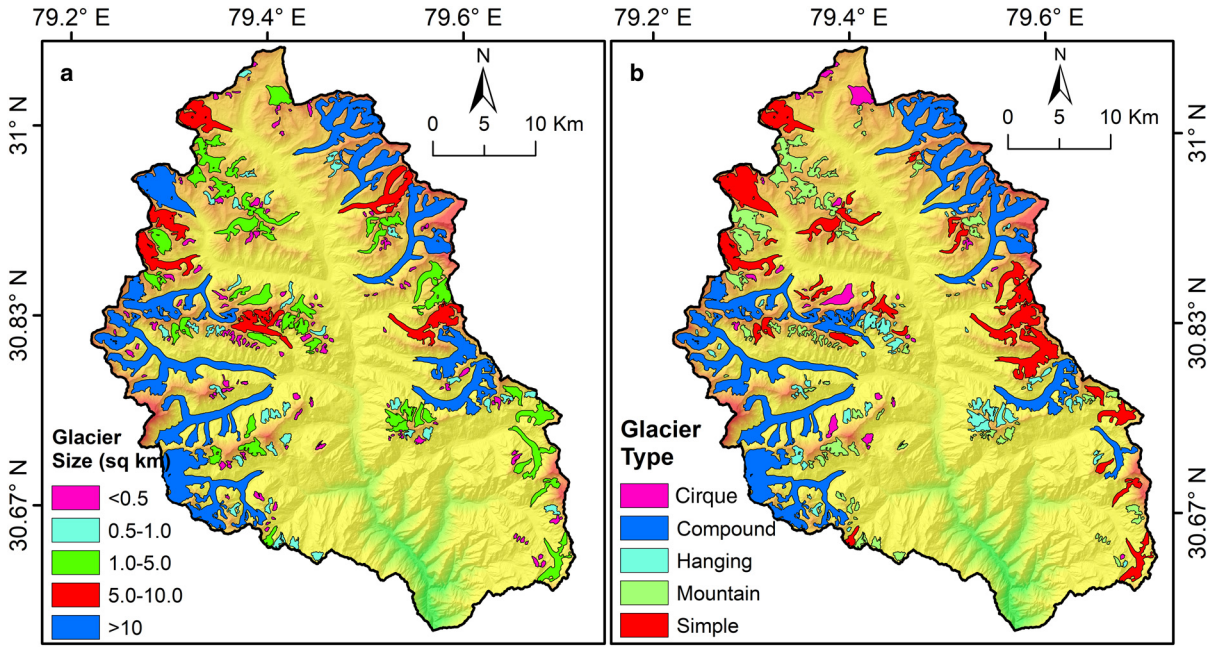

Fig. 6. The distribution of glaciers of UAB: (a) based on their size and (b) based on their morphology.

https://doi.org/10.1017/jog.2022.87 Published online by Cambridge University Press

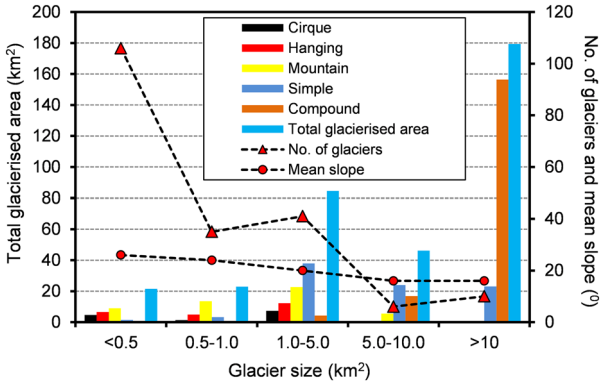

Fig. 7. Distribution of number of glaciers, total glacierised area and mean slope for each area range and morphological type.

In terms of the glacier morphology, mountain glaciers experienced the highest area losses (10.6%), followed by hanging glaciers (~9.2%) and cirque glaciers (~8.6%) (Supplementary Table S2). Out of the 175 glaciers analysed for area change during 1994–2020, 113 were debris-free. During this period, the total area of debris-covered glaciers reduced from 305.3 ± 7.6 to $296.6 \pm 4.4\ km^2$ corresponding to $2.9 \pm 2.9\%$ ($0.11 \pm 0.11\%\ a^{-1}$) whereas the relative area loss of the debris-free glaciers was $10.8 \pm 2.8\%$ ($0.42 \pm 0.11\%\ a^{-1}$).

The area changes of 138 glaciers were analysed for the periods 1994–2006 and 2006–2020. The total area of these glaciers was $332.4 \pm 8.3\ km^2$ in 1994, $326.8 \pm 6.9\ km^2$ in 2006 and $319.5 \pm 4.8\ km^2$ in 2020. Hence, the total area change during the periods was $-1.7 \pm 3.2\%$ ($-0.14 \pm 0.27\%\ a^{-1}$) during 1994–2006, and $-2.2 \pm 2.6\%$ ($-0.16 \pm 0.19\%\ a^{-1}$) during 2006–2020. While the mean value of the area loss has slightly increased in the period 2006–2020 as compared to 1994–2006, no significant trend can be inferred.

6.3. Length changes

The length of all 20 glaciers studied decreased during the period 1994–2020 with an average retreat rate of $11.4 \pm 1.8\ m\ a^{-1}$. The retreat rate of individual glaciers varied considerably between $4.6 \pm 1.8\ m\ a^{-1}$ (Arwa 01 Glacier) and $18.9 \pm 1.8\ m\ a^{-1}$ (Khuliya Garvya Glacier) (Fig. 10). The average retreat rate of the 18 glaciers which are covered in all the three scenes was $9.6 \pm 1.9\ m\ a^{-1}$ during 1994–2006 and $14.9 \pm 1.2\ m\ a^{-1}$ during 2006–2020. For two of the 18 glaciers, the retreat rate increased during 2006–2020 as compared with that of 1994–2006. The retreat rate of Bhagirath Kharak (glacier number 3 in Fig. 1) increased quite significantly from $4.9 \pm 1.9\ m\ a^{-1}$ during 1994–2006 to $16.0 \pm 1.2\ m\ a^{-1}$ during 2006–2020. Thus, it can be inferred that the retreat rate of the large glaciers in the basin has significantly increased in the period 2006–2020 as compared to 1994–2006.

6.4. Debris cover changes

The debris-covered area of the studied 175 glaciers increased from $80.1 \pm 2.8\ km^2$ in 1994 to $90.8 \pm 2.2\ km^2$ in 2020, corresponding to a rate of increase of $0.52 \pm 0.17\%\ a^{-1}$. For the 138 glaciers measured in 1994, 2006 and 2020, the debris cover increased from $65.1 \pm 2.3\ km^2$ (21.0%) in 1994 to 67.5 ± 1.9 (21.8%) in 2006 to $73.3 \pm 1.8\ km^2$ (24.7%) in 2020. The percentage of increase corresponding to the debris cover was $0.31 \pm 0.38\%\ a^{-1}$ (1994–2006), $0.61 \pm 0.27\%\ a^{-1}$ (2006–2020) and $0.49 \pm 0.17\%\ a^{-1}$ for the whole study period (1994–2020). Thus, the rate during 2006–2020 was significantly larger than 1994–2006. Interestingly, small glaciers ($<5\ km^2$) showed a higher ($0.81 \pm 0.18\%\ a^{-1}$) rate of increase in the extent of debris cover as compared to $0.44 \pm 0.06\%\ a^{-1}$ for large glaciers ($>5\ km^2$) during the study period 1994–2020.

6.5. Climatic trends in UAB

Our analysis of the CRU temperature and precipitation data shows that the mean annual temperature (MAT) increased by 0.5°C during 1901–2019 (Fig. 11a). An accelerated warming rate of ~$0.04°C\ a^{-1}$ occurred after 1990 (Supplementary Table S3 and Fig. S2). Moreover, the winter temperature increased at a slightly higher rate ($0.041°C\ a^{-1}$) as compared to the summer temperature ($0.036°C\ a^{-1}$) for the period between 1990 and 2019. Overall, decreasing precipitation rates were found from 1901 to 2019 (Fig. 11b), though reduction was noticed in winter precipitation particularly since 1990 (Supplementary Fig. S2). It is further observed that summer precipitation increased (40 mm per decade) while winter precipitation slightly decreased (~10 mm per decade) from 1990 to 2019. However, there is a decreasing trend from ~1970 to ~2000 and then an increasing trend till 2019.

7. Discussion

7.1. Comparison with other inventories

We compare our UAB inventory with other existing ones such as the inventory compiled by GSI (Raina and Srivastava, 2008), the Randolph Glacier Inventory (RGI) v6.0 (RGI Consortium, 2017), International Centre for Integrated Mountain Development (ICIMOD) (Bajracharya and Shrestha, 2011) and Glacier Area Mapping for Discharge from the Asian Mountains Glacier Inventory, version 2.0 (GGI2) (Sakai, 2019). All these were generated at different epochs, using different datasets and mapping

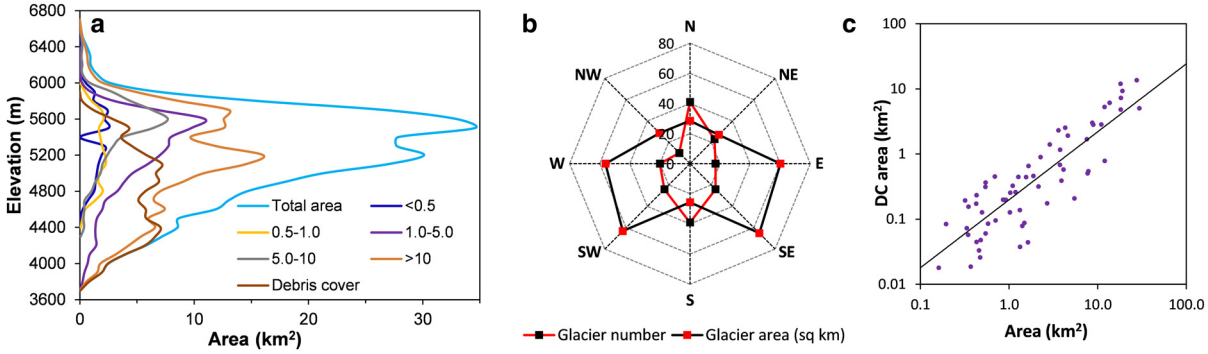

Fig. 8. (a) Area-elevation distribution of all glaciers (blue) and of the glaciers in different size ranges (other colours). (b) Distribution of glacier number and glacierised area at different orientations. (c) Debris-covered area plotted against the total glacier area.

https://doi.org/10.1017/jog.2022.87 Published online by Cambridge University Press

Table 4. Area loss of 175 glaciers from 1994 to 2020 according to their size

Glacier size (km^2)	Number	Total glacier area (km^2)		Area change (km^2)	Fractional change (%)	Change rate (% a^{-1})
		1994	2020			
<0.5	88	22.8 ± 1.1	19.3 ± 0.6	−3.5 ± 1.3	−15.5 ± 5.7	−0.60 ± 0.22
0.5–1.0	34	25.5 ± 0.8	22.8 ± 0.3	−2.7 ± 0.8	−10.5 ± 3.3	−0.40 ± 0.13
1.0–5.0	37	86.6 ± 1.7	81.4 ± 1.1	−5.2 ± 2.0	−6.0 ± 2.3	−0.23 ± 0.09
5.0–10	6	48.0 ± 0.7	46.3 ± 0.4	−1.7 ± 0.9	−3.6 ± 1.8	−0.14 ± 0.07
>10	10	185.7 ± 2.4	183.3 ± 1.5	−2.5 ± 2.8	−1.3 ± 1.5	−0.05 ± 0.06
<5	158	134.9 ± 4.7	123.4 ± 3.1	−11.5 ± 5.7	−8.5 ± 4.2	−0.33 ± 0.16
>5	17	233.8 ± 3.2	229.6 ± 2.0	−4.2 ± 3.7	−1.8 ± 1.6	−0.07 ± 0.06
Total	175	368.6 ± 9.2	353.0 ± 12.2	−15.6 ± 10.6	−4.2 ± 2.9	−0.16 ± 0.11

techniques. The RGI 6.0, ICIMOD and GGI2 inventories were derived from Landsat images acquired between 1999 and 2003 (i.e. 2001 ± 2), 2002 and 2008 (i.e. 2005 ± 3) and between 1999 and 2010 (i.e. 2005 ± 5) respectively. These are available in digital format (vector shapefiles) (Supplementary Fig. S3a). The inventory of GSI was prepared on 1 : 50 000 scale, using survey of India (SOI) topographic maps (1962). It was supplemented with satellite imageries (1990s) and aerial photographs (2000) wherever available (Sangewar and Shukla, 2009). The GSI inventory provides primary information of glaciers but unfortunately is not available in the digital format (Braithwaite, 2009). Therefore, we have used the data extracted from the publication of Raina and Srivastava (2008).

The total glacierised area of RGI (354.0 km^2), ICIMOD (354.8 km^2) and of our inventory (354.6 km^2) is approximately the same but that of GSI (436.9 km^2) and GGI2 (410.5 km^2) is significantly larger. The total number of glaciers in our inventory (198) is smaller than the RGI (223), ICIMOD (338) and GGI2 (318) inventories but larger than the GSI (159) (Supplementary Table S4).

We assume that the difference in the total area and number of glaciers between our inventory and the others is primarily due to (a) the difficulty in distinguishing between snow and ice, (b) the difficulty in delineating the boundary of debris-covered glaciers, apart from the different dates of the data sources.

For example, two well-separated glaciers, Satopanth and Bhagirath Kharak (where we do our fieldwork), are marked as a single glacier in all the above inventories (Supplementary Fig. S3d). The SOI topographic map (1962) shows the Bhagirath Kharak and Satopanth glaciers as a single glacier, presumably the reason why the GSI inventory counts them as a single glacier. Nainwal and others (2016) pointed out that this was not the case and that the inaccuracy of the SOI map was probably because of the difficulty of distinguishing between ice and snow. We are uncertain why the two glaciers are counted as one in the other inventories. However, the outwash plain of these two glaciers has a large number of dead ice mounds, moraines and debris deposits. Hence, it is difficult to identify the outlines correctly without local knowledge.

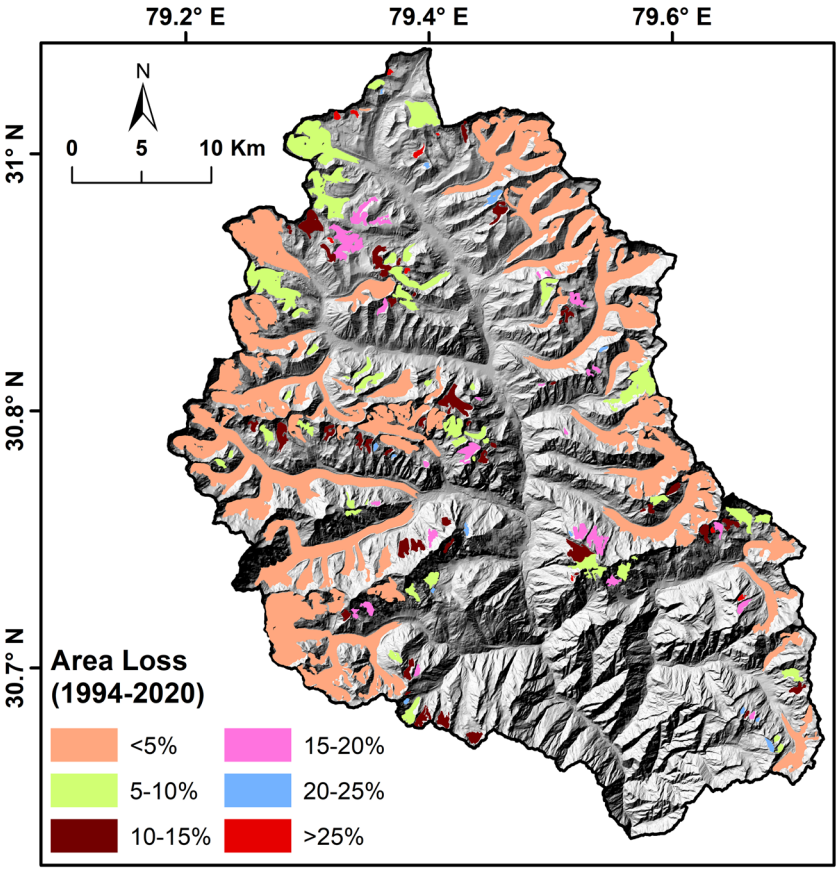

Fig. 9. The distribution of the area loss of 175 glaciers in the basin during the period 1994–2020.

https://doi.org/10.1017/jog.2022.87 Published online by Cambridge University Press

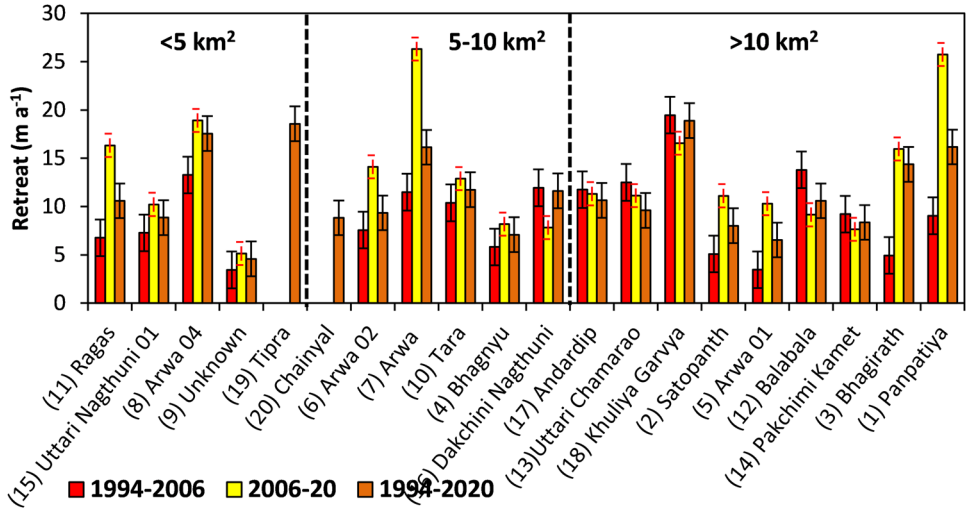

Fig. 10. Retreat rates of the 20 investigated glaciers for the periods 1994–2006, 2006–2020 and 1994–2020. For numbering see Figure 1.

The main discrepancy in the total number of glaciers comes from the number of small glaciers (<0.5 km^2). By superimposing available shapefiles of RGI6.0, ICIMOD and GGI2 over our glacier outlines, we find that the differences occur mainly due to the inclusion of seasonal snow ice patches at the mountain slopes, problems of the separation of glaciers at ice divide due to DEM inaccuracies at steep slopes, mistaking avalanche cones for glaciers and difficulties in demarcation of debris-covered ice (Supplementary Fig. S3b).

Overall, we feel that our manual method of visually interpreting the Sentinel-2 images (10 m spatial resolution) at 5-day intervals during September and October with input from high-resolution Google Earth images (0.5–2.5 m) along with field validation makes our results more reliable than that of the other inventories for the limited region, namely the UAB.

7.2. Comparison with other studies within the UAB

Our results have been compared with the previous study on Satopanth and Bhagirath Kharak glaciers of UAB (Nainwal and others, 2016). The rate of area vacated in the frontal region of these two glaciers during the period 1980–2013 was estimated to be 0.0048 ± 0.001 and 0.0027 ± 0.001 km^2 a^{-1} respectively (Nainwal and others, 2016). In our present work, the rate of area loss at the frontal parts for 1994–2020 was found to be 0.0052 ± 0.022 and 0.0061 ± 0.033 km^2 a^{-1}. Thus, our remote-sensing estimates of the area loss of Satopanth Glacier are consistent within the uncertainties with the field measurements. The minor difference in Bhagirath Kharak Glacier could be due to significant changes in the snout morphology observed in the field after 2015.

The same is true for the length changes. Based on the sketch map (1956) and field survey (2013), Satopanth and Bhagirath Kharak glaciers have retreated at an average rates of 5.7 ± 0.6 and 6.0 ± 0.9 m a^{-1} respectively during 1956–2013 (Nainwal and others, 2016). The authors also reported an increase (7.2 ± 3.0 m a^{-1}) in the retreat rates for the period 1980–2005 as compared to 5.2 ± 3.7 m a^{-1} during 2005–2013. This is, hence, in line with our observations.

The area loss of the three large glaciers in UAB, Tara, Tipra and Khulia Garvya, reported by Garg and others (2017) shows the same rate of area loss as our study. However, the rate of area loss of Panpatiya Glacier, reported by them, is significantly larger ($0.08 \pm 0.03\%$ a^{-1}) than what we have observed ($0.04 \pm 0.13\%$ a^{-1}). This inconsistency may be due to differences in the demarcation of complex glacier front since there is a large amount of debris flow from the lateral moraines and the shadowing effect resulting from clouds and narrow valley.

We have estimated the retreat rate of Tipra Glacier for the period 1994–2020 to be 18.6 ± 1.8 m a^{-1}. This is consistent with Garg and others (2017) who report 17.8 ± 2.5 m a^{-1} for the period of 1994–2015. It is also consistent with the reported rates of Mehta and others (2011): 13.4 m a^{-1} during 1962–2002 and 21.3 m a^{-1} during 2002–2008.

Our estimates of the retreat rates of Tara (10) and Khuliya Garvya (18) glaciers are in generally in agreement with the results reported by Garg and others (2017). They reported a retreat rate of Tara Glacier to be 24.6 ± 2.5, 37 ± 7.3 and 12 ± 3.7 m a^{-1} during 1994–2015, 1994–2001 and 2001–2015 respectively. Our

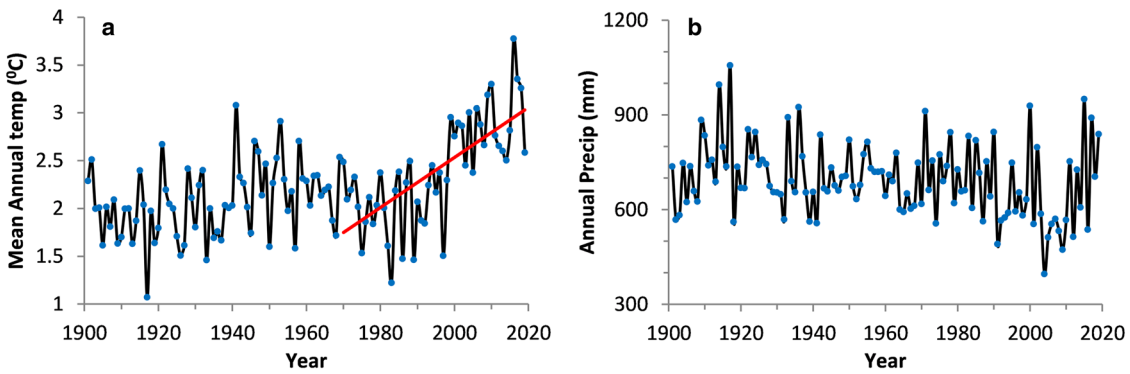

Fig. 11. (a) Mean annual temperature and (b) precipitation, CRU data (1901–2019). Red line indicates the linear increasing trend in MAT from 1970 to 2019.

https://doi.org/10.1017/jog.2022.87 Published online by Cambridge University Press

Table 5. Comparison of area loss (% a^{-1}) and debris cover change (% a^{-1}) with previous studies in the Himalaya

S. No.	Basin/study area	Glacier No.	Area (km^2)	Period	Data used	Area change rate (% a^{-1})	Debris cover change (% a^{-1})	Study
Central Himalaya								
1	**Upper Alaknanda**	**175**	**353.0**	**1994–2020**	**Landsat TM and Sentinel**	**0.16**	**0.52**	**Present study**
	Basin	**138**	**326.8**	**1994–2006**	**Landsat TM and ASTER**	**0.14**	**0.31**	
			319.5	**2006–2020**	**ASTER and Sentinel**	**0.16**	**0.61**	
2	Alaknanda	75	306.35	1968–2006	Corona and ASTER	0.15	0.47	Bhambri and others (2011*a*)
		24	78.90	1990–2006	Landsat and ASTER	0.36	1.29	
3	Bhagirathi	13	266.17	1968–2006	Corona and ASTER	0.09	0.31	
		5	11.54	1990–2006	Landsat TM and ASTER	0.42	3.18	
4	Uttarakhand	18	306.40	1994–2015	Landsat TM and OLI	0.09	0.55	Garg and others (2017)
5	Bhilangana	33	80.34	1968–2014	Corona and Cartosat	0.22	–	Raj and others (2017)
6	Dhauliganga	15	68.00	1968–2016	Corona and Landsat OLI	0.14	–	Sattar and others (2019)
7	Khumbu region, Nepal	–	87.39	1962–2005	Corona and ASTER	0.12	0.06	Bolch and others (2008)
				1992–2005	Landsat Tm and ASTER	0.20	0.10	
				1962–2011	Corona and Landsat ETM+	0.27	0.36	Thakuri and others (2014)
				1992–2011	Landsat TM and ETM+	0.43	0.73	
Western Himalaya								
8	Tirungkhad	20	32.93	1965–2018	Corona and Sentinel	0.11	–	Mandal and Sharma (2020)
				1990–2018	Landsat Tm and Sentinel	0.11	–	
9	Baspa	97	186.2	1972–2011	Landsat MSS and TM	0.51	1.8	Mir and others (2017)
				1992–2011	Landsat TM	0.55	1.6	
10	Ravi	159	119.9	1971–2013	Corona and Landsat OLI	0.11	0.47	Chand and Sharma (2015)
		54	67.4	1989–2013	Landsat TM and OLI	0.14	0.17	
11	Jankar Chhu	131	181.4	1971–2016	Corona and Sentinel	0.14	1.0	Das and Sharma (2018)
	Watershed Bhaga	44	155.8	1989–2016	Landsat Tm and Sentinel	0.16	2.2	
12	Chandra	171	608.1	1971–2016	Corona and Sentinel	0.11	0.69	Sahu and Gupta (2020)
		34	537.8	1989–2016	Landsat and Sentinel	0.08	0.41	
		15	377.7	1980–2010	Landsat MSS and LISS III	0.08	–	Pandey and Venkataraman (2013)
		–	944	1971–2015	Corona and Landsat OLI	0.03		Mukherjee and others (2018)
13	Miyar	29	227	1989–2014	Landsat TM and OLI	0.15	–	Patel and others (2018)
14	Laddakh	657	308.9	1991–2014	Landsat TM and OLI	0.56	–	Chudley and others (2017)
		121	82.6	1969–2010	Corona and Landsat TM	0.35	–	Schmidt and Nüsser (2012)
		97	75.2	1991–2010	SPOT and Landsat TM	0.39	–	
15	Zanskar	5	247.58	1977–2013	Landsat MSS and OLI	0.42	0.78	Shukla and Qadir (2016)
16	Shuru	240	481	1971–2017	Corona and Landsat OLI	0.13	1.3	Shukla and others (2020)
Eastern Himalaya								
17	Teesta	38	195.31	1989–2010	Landsat TM and ETM+	0.16	–	Basnett and others (2013)
18	Sikkim	186	569	1962–2000	Corona and Landsat ETM+	0.52	–	Racoviteanu and others (2015)

estimates, for the retreat of the same glacier, are 10.4 ± 1.9 m a^{-1} for 1994–2006 but match well for the second (12.9 ± 1.2 m a^{-1} for 2006–2020). For Khuliya Garvya Glacier, Garg and others (2017) reported a retreat rate of 26.9 ± 2.5 m a^{-1} during 1994–2015; whereas our estimate is 18.9 ± 1.8 m a^{-1} during 1994–2020. The area change of this glacier is similar in Garg and others (2017) and our study. Therefore, we could expect the difference in retreat rates being due to different demarcation of parallel flow lines used for length change or retreat estimation. The glacier is arc-shaped and of irregular front (Figs 3b, e).

Overall, while there are inconsistencies in case of a few individual glaciers, all the studies indicate that the glaciers in the region are retreating with varying rates and that these rates have on average increased in the past decade.

7.3. Comparison of area and debris cover change with other Himalayan basins

Table 5 collates the results of the studies that estimate the rate of fractional loss of area and the rate of change of fractional debris cover in the various glacierised basins across the Himalaya (i.e. Western, Central and Eastern regions). These regions have different climatic and topographic settings. The comparative analysis of glacier area changes of UAB with other Himalayan basins has been done on the basis of time window and used satellite data; and indicates that the glaciers in UAB have shrunk at rates analogous to those of the other studies.

Das and Sharma (2018) reported the glaciers in Jankar Chhu watershed, Chandrabhaga (Chenab) Basin, had lost area at a rate of $0.16 \pm 0.1\%$ a^{-1} during 1989–2016. The Jankar Chhu watershed has 83 debris-covered glaciers, out of 153 glaciers in the basin. The majority of glaciers (94) are small in size (<0.5 km^2). The glaciers of Ravi Basin, Western Himalaya were studied by Chand and Sharma (2015) who estimated a loss rate of $0.16 \pm 0.4\%$ a^{-1} during 1989–2010. Patel and others (2018) reported a similar loss rate of $0.16 \pm 0.0\%$ a^{-1} for the Miyar Basin, during 1989–2014. These results are the same as what we observed in the UAB.

However, there are some basins in the western Himalaya, where a higher area loss rate has been reported. For example, Mir and others (2017) reported a loss rate of 0.51 ± 0.01 a^{-1} during 1976–2011 in the Baspa Basin. One reason for the higher rates may be due to the use of coarse resolution (60 m) Landsat MSS image; while Mandal and Sharma (2020) observed area loss of 5.6% (0.11% a^{-1}) in the adjacent Tirungkhad watershed, based on relatively high-resolution Corona (1965) and Sentinel (2018) images. Chudley and others (2017) reported a loss of 45.3 km^2 (12.8% or 0.52% a^{-1}) in Ladakh range during 1991 and 2014. The difference may be due to exceptionally small size of glaciers and their characteristic (morphology) in this range (Schmidt and Nüsser, 2012). In the Eastern Himalaya, a loss rate of 0.16

https://doi.org/10.1017/jog.2022.87 Published online by Cambridge University Press

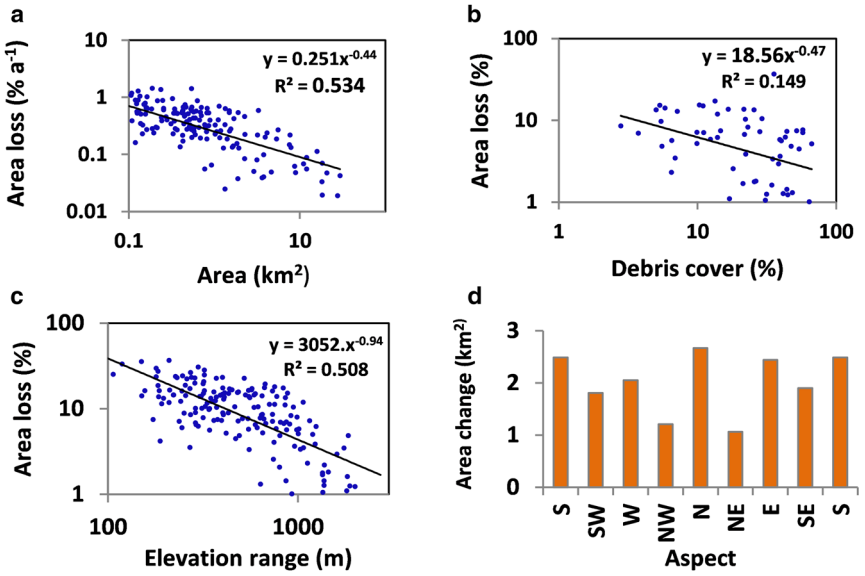

Fig. 12. Scatter plots showing the correlation between area loss (%) during the study period (1994–2020) and non-climatic parameters; (a) glacier area, (b) debris cover %, (c) elevation range, (d) area loss vs aspect.

± 0.3% a^{-1} was reported in the Tista basin, during 1989–2010 by Basnett and others (2013).

Overall, given the uncertainties (wherever estimated) in the rate of loss of glacierised area, all the studies seem to indicate that the rate in UAB is roughly the same as that in the rest of Himalaya, namely, ~0.1–0.2% a^{-1}. However, there may be exceptional regions in the western Himalaya where it may be significantly higher.

There were significant changes in the extent of debris cover in the UAB. The rate of change of the fraction of debris cover area in UAB was significantly higher (0.61% a^{-1}) in the period 2006 and 2020 as compared to 0.31% a^{-1} from 1994 to 2006. The earlier study in UAB observed the similar (0.46% a^{-1}) rate of increase of the debris cover during 1968–2006 (Bhambri and others, 2011*a*). However, the rate was significantly larger (1.3% a^{-1}) for the period between 1990 and 2006. This may be due to the fact that only 24 glaciers were accounted. Garg and others (2017) report a rate of 0.6% a^{-1} during 1994–2015 based on 18 glaciers in the Central Himalaya, similar to our results. Overall, the rate of debris-cover increase we report is comparable to the previous studies in the Himalaya (Table 5).

7.4. Regional climatic trends and their impact on glacier change

Climate fluctuations are key to understand glacier variability, the main factors being temperature and precipitation (Oerlemans, 2005). While field data close to glaciers are scarce, there are some weather stations in the Himalaya from where data have been reported. To summarise, in the period 1866–2010, an increase in temperature, varying between ~0.1 and ~1°C, and a decrease in precipitation have been reported (Basistha and others, 2009; Bhutiyani and others, 2010; Shrestha and Aryal, 2011; Singh and others, 2013). This is consistent with our analysis of the CRU data plotted in Figure 11. However, we note that after ~2000–2010, the CRU data show a sharp increase in precipitation.

The above discussion motivated us to attempt to interpret the overall changes in the glacier lengths and areas that we observe based on the following regional climate scenario: (a) the regional temperature and precipitation started showing significant positive trends after ~1960–80, (b) the regional temperature increased rapidly in the past three decades or so at a rate of 3–4°C per century, and (c) the regional precipitation decreased from ~1960 to 2010 and then rapidly increased till 2020.

Combining our results with the previous study in UAB by Bhambri and others (2011*a*) we conclude that the total glacierised area has decreased from 1968 to 2020 at a constant fractional rate of ~0.015% a^{-1}. This is probably a combined effect of the increase in temperature and decrease in precipitation during this period. Disentangling the two effects requires a basin scale model of the glacier dynamics which we do not attempt. We also observed that average retreat rate of the large UAB glaciers increased from 9.3 ± 1.9 m a^{-1} (1994–2006) to 13.3 ± 1.8 m a^{-1} (2006–2020). The length of a glacier responds to temperature changes much quicker than to precipitation changes (Oerlemans, 2005). Basically, the temperature changes dominantly affect the ablation zone whereas precipitation changes dominantly affect the accumulation zone. Consequently, it takes time for precipitation changes to reflect in length changes. The response time of length to temperature changes varies from glacier to glacier depending on its size, slope and extent of debris cover (Oerlemans, 2005, Banerjee and Shankar, 2013). Our interpretation of the increase in the average retreat rate is that it was dominantly controlled by the warming. The glaciers with larger response times took longer to respond to the changes. Hence, the average retreat rate increased in time and, even though the area and length changes show a delayed response to climate forcing it is evident that the atmospheric warming was the main driver of the glacier wastage in UAB and the whole Himalaya. Long-term high altitude in-situ meteorological records in the basin along with ground-based glaciological measurements (e.g. mass balance, debris thickness) are needed to provide insights on overall glacier response and establish a better relation between glacier changes and climatic parameters.

7.5. Role of glacier-specific factors on area loss

To understand the basin scale area loss, we need to understand the area loss rates of individual glaciers as a function of their attributes since glaciers respond heterogeneously even under similar climatic conditions (Salerno and others, 2017; Brun and others, 2019). We have attempted to do this by plotting the relative area loss rates of the glaciers in UAB against several non-climatic attributes (area, debris cover fraction, elevation range and aspect, Fig. 12).

All the glaciers of UAB show a loss of area between 1994 and 2020. The area loss of individual glaciers ranges from 0.5 to 38%, with a total loss of 4.2 ± 2.9% (0.16 ± 0.11% a^{-1}). This heterogeneous behaviour of glaciers is probably owing to the interplay

https://doi.org/10.1017/jog.2022.87 Published online by Cambridge University Press

between topographic and climatic variables. Glacier area loss in UAB is dependent on glacier size and we found a significant negative correlation ($r = -0.73$) with coefficient of determination (R^2) of 0.53 between area loss (%) and glacier area (size) (Fig. 12a). Similar trends were noticed in the previous studies in Himalaya indicating sensitivity of smaller glaciers to climate change (Kulkarni and others, 2007; Bolch and others, 2012; Chand and Sharma, 2015). Such small glaciers have short response time and usually adjust their geometry instantly (Huss and Fischer, 2016). Despite the good correlation between area loss and glacier size in UAB, it is slightly lower than other basins (e.g. Ravi, Miyar, Baspa, Shyok and Jankar) which may be because of relatively higher (1.2 km^2) mean glacier size in UAB than these Himalayan basins.

The debris cover of a glacier strongly influences its ablation process. The increasing rate of debris-cover extent over the glaciers is common for shrinking glaciers (Benn and others, 2012; Bolch and others, 2012; Kirkbride and Deline, 2013) due to avalanching activity in upper reaches of glacier catchment (Scherler and others, 2011; Laha and others, 2017) and the up-glacier shift of SLA (Shukla and Garg, 2020). The debris-cover area expands up glacier over the time and slowdown the glacier melting (Dobhal and others, 2013; Pratap and others, 2015; Shah and others, 2019), however such glaciers lose mass mainly by thinning not retreat (Banerjee and Shankar, 2013; Ragettli and others, 2016; Remya and others, 2020). Therefore, we may expect the area loss rate to decrease with increasing fraction of debris cover. A negative correlation ($R^2 = 0.15$) between glacier area loss and debris-covered fraction was indeed seen (Fig. 12b). Debris-covered glaciers have lost 2.9 ± 2.6% of their area compared to the 10.8 ± 2.8% loss of the debris-free ones. Similar pattern of area loss of debris-covered glaciers was observed in the other Himalayan basin; for example, Sahu and Gupta (2020) reported area loss of ~3% for debris-covered glaciers in comparison with 11% clean ice glaciers in Chanda Basin. Likewise, Mir and others (2017) observed area change of debris-covered glaciers to be 14% only in Baspa Basin while clean glacier lost an area of 27% during the studied period.

The vertical extent of a glacier is described by its elevation range and mean elevation. The slope of a glacier is derived by dividing the elevation range by its length. Therefore, these two parameters are related to each other. The loss rate is plotted against the elevation range in Figure 12c and good negative correlation (R^2 −0.51) was recorded. Thus, within the uncertainties, the loss rate is inversely proportional to the elevation range. Glaciers with larger elevation ranges will tend to have larger areas and consequently it is not surprising that the loss rate decreases with the increasing elevation range. However, the exponent for the area is ~0.6 whereas for the elevation range it is ~−1. This indicates that the slope plays a significant role in the dynamics.

As expected, the rate of area loss strongly correlates with the aspect as found elsewhere (e.g. DeBeer and Sharp, 2009) (Fig. 12d). The north-south flowing glaciers have been shrinking faster than those flowing east-west. The loss rate of north-facing glaciers was 0.36 ± 0.11% a^{-1} and it was 0.34 ± 0.11% a^{-1} for those facing the south. On the contrary, the loss rate of the NW and NE facing glaciers was 0.13 ± 0.11 and 0.15 ± 0.11% a^{-1} respectively. Similar behaviour has been reported in the previous studies in Alaknanda Basin (Nainwal and others, 2008; Bhambri and others, 2011*a*). Also, Das and Sharma (2018) and Sahu and Gupta (2020) found a similar dependence of the area loss on the aspect in Jankar Chhu and Chandra basins, Western Himalaya.

To summarise, the average response of individual glaciers as a function of their non-climatic attributes is typically non-linear. To our knowledge, all past studies (Bhambri and others, 2011*a*; Chand and Sharma, 2015; Garg and others, 2017; Das and Sharma, 2018; Sahu and Gupta, 2020; Shukla and others, 2020) have analysed this issue using linear regression techniques. Our analysis seems to show that this may not be adequate. We feel that more detailed work needs to be done on this issue.

8. Conclusions

We presented an updated glacier inventory for the UAB for 2020 using Sentinel-2 images and reported the glacier changes in the basin from 1994 to 2020. The updated inventory contains 198 glaciers and shows that the total glacierised area was 354.6 ± 8.5 km^2 in 2020.

The glacierised area in the UAB reduced by 15.6 ± 10.6 km^2 from 368.6 ± 9.2 km^2 in 1994 to 353.0 ± 5.3 km^2 in 2020. This implies an average loss rate of 0.16 ± 0.11% a^{-1} during this period.

Based on the observations of 138 glaciers, a similar rate of area loss was estimated for the time periods, 1994–2006 and 2006–2020 (0.14 ± 0.27 and 0.16 ± 0.19% a^{-1}). According to glacier morphology, the highest area changes were shown by mountain glaciers (10.6%), followed by hanging glaciers (9%) and cirques (8.6%). A significant increase in debris-covered area (13.4 ± 4.4%) was observed during the study period. The retreat of the 20 observed glaciers varied from 4.6 ± 1.8 to 18.9 ± 1.8 m a^{-1}. The average glacier retreat rates increased by ~30% from 9.3 ± 1.9 m a^{-1} (1994–2006) to 13.3 ± 1.8 m a^{-1} during the last decade (2006–2020).

The CRU data for the MAT show that warming rates increased to 0.04°C a^{-1} (for the period 1990–2020) from 0.001°C a^{-1} (1901–1990) in UAB. Further, a rate of warming of 0.026°C a^{-1} was observed during 1970–2019. Glacier size, debris-cover extent, elevation range and aspect are found controlling glacier-specific factors for the fractional rate of area loss in UAB from 1994 to 2020. We hope that our data analysis results will motivate modellers to develop physically based models which will eventually result in reliable future projections at a basin scale.

Supplementary material. The supplementary material for this article can be found at https://doi.org/10.1017/jog.2022.87.

Acknowledgements. The field work at Satopanth Glacier was supported by SERB & DST, New Delhi (Grant No. SB/DGH-101/2015 and DST/CCP/NHC/158/2018), IMSc, Chennai and SAC-ISRO funded projects. Parts of the work were conducted in the framework of the project 'Understanding and quantifying the transient dynamics and evolution of debris-covered glaciers' funded by the Swiss National Science Foundation (Grant No. 200021-169775). HCN, AM & SS are thankful to the Vice-Chancellor, HNB Garhwal University to provide infrastructural facilities. AM is grateful to Dr Prabhat Semwal for his help in GIS-related issues, and to Dr Argha Banerjee and Dr D. P. Dobhal for their valuable suggestions and discussion during the work. We also acknowledge the USGS (Earth Explorer), European Space Agency (ESA), NASA's Earth Data, and the RGI working group, ICIMOD and A. Sakai (GGI2) for providing satellite images, and other relevant data such as the glacier inventories free of cost. We thank Dr. Rachel Carr, Scientific Editor, and the anonymous reviewers for their valuable comments and suggestions which led to the present improved manuscript.

Author contributions. AM conceptualised the work along with HCN and RS, performed all analysis and wrote the first draft. HCN and RS supervised the research work. T B provided guidance to improve the quality of work. Field work is supported by SSS. All the authors contributed to the final form of the article.

Conflict of interest. None.

References

Azam MF and 5 others (2018) Review of the status and mass changes of Himalayan-Karakoram glaciers. *Journal of Glaciology* **64**(243), 61–74. doi: 10.1017/jog.2017.86.

Azam MF and 12 others (2021) Glaciohydrology of the Himalaya-Karakoram. *Science* **373**(6557). doi: 10.1126/science.abf3668.

Bajracharya B and Shrestha SR (eds) (2011) *The Status of Glaciers in the Hindu Kush–Himalayan Region*. Kathmandu: International Centre for Integrated Mountain Development.

Bandyopadhyay D, Singh G and Kulkarni AV (2019) Spatial distribution of decadal ice-thickness change and glacier stored water loss in the Upper Ganga basin, India during 2000–2014. *Scientific Reports* **9**(1), 1–9. doi: 10.1038/s41598-019-53055-y.

Banerjee A and Shankar R (2013) On the response of Himalayan glaciers to climate change. *Journal of Glaciology* **59**(215), 480–490. doi: 10.3189/2013JoG12J130.

Basistha A, Arya DS and Goel NK (2009) Analysis of historical changes in rainfall in the Indian Himalayas. *International Journal of Climatology* **29** (4), 555–572. doi: 10.1002/joc.1706.

Basnett S, Kulkarni AV and Bolch T (2013) The influence of debris cover and glacial lakes on the recession of glaciers in Sikkim Himalaya, India. *Journal of Glaciology* **59**(218), 1035–1046. doi: 10.3189/2013JoG12J184.

Benn DI and 9 others (2012) Response of debris-covered glaciers in the Mount Everest region to recent warming, and implications for outburst flood hazards. *Earth Science Reviews* **114**(1–2), 156–174. doi: 10.1016/j.earscirev.2012.03.008.

Bhambri R, Bolch T and Chaujar RK (2011*b*) Mapping of debris-covered glaciers in the Garhwal Himalayas using ASTER DEMs and thermal data. *International Journal of Remote Sensing* **32**(23), 8095–8119. doi: 10.1080/01431161.2010.532821.

Bhambri R, Bolch T and Chaujar RK (2012) Frontal recession of Gangotri Glacier, Garhwal Himalayas, from 1965 to 2006, measured through high resolution remote sensing data. *Current Science* **102**(3), 489–494. doi: 10.5167/uzh-59630.

Bhambri R, Bolch T, Chaujar RK and Kulshreshtha SC (2011*a*) Glacier changes in the Garhwal Himalaya, India, from 1968 to 2006 based on remote sensing. *Journal of Glaciology* **57**(203), 543–556. doi: 10.3189/002214311796905604.

Bhattacharya A and 8 others (2021) High Mountain Asian glacier response to climate revealed by multi-temporal satellite observations since the 1960s. *Nature Communications* **12**(4133). doi: 10.1038/s41467-021-24180-y, 2021.

Bhutiyani MR, Kale VS and Pawar NJ (2010) Climate change and the precipitation variations in the northwestern Himalaya: 1866–2006. *International Journal of Climatology* **30**(4), 535–548. doi: 10.1002/joc.1920

Bolch T and 7 others (2010*a*) A glacier inventory for the western Nyainqentanglha Range and the Nam Co Basin, Tibet, and glacier changes 1976–2009. *The Cryosphere* **4**(3), 419–433. doi: 10.5194/tc-4-419-2010.

Bolch T and 11 others (2012) The state and fate of Himalayan glaciers. *Science* **336**(6079), 310–314. doi: 10.1126/science.1215828.

Bolch T (2017) Asian glaciers are a reliable water source. *Nature* **545**(7653), 161–162. doi: 10.1038/545161a.

Bolch T and 11 others (2019) Status and change of the cryosphere in the extended Hindu Kush Himalaya region. In Wester P, Mishra A, Mukherji A and Shrestha AB (eds), *The Hindu Kush Himalaya Assessment: Mountains, Climate Change, Sustainability and People*. Cham: Springer International Publishing, pp. 209–255. Available at doi: 10.1007/978-3-319-92288-1_7.

Bolch T, Buchroithner M, Kunert A and Kamp U (2007) Automated delineation of debris-covered glaciers based on ASTER data. *Geoinformation in Europe (Proceedings of 27th EARSel Symposium, 04–07 June 2007), Bozen, Italy*. (June), pp. 403–410 citeulike-article-id:9343684%5Cn. Available at http://web.unbc.ca/~bolch/publications/BolchAl07_EARSeL-iPr.pdf.

Bolch T, Buchroithner M, Pieczonka T and Kunert A (2008) Planimetric and volumetric glacier changes in the Khumbu Himal, Nepal, since 1962 using Corona, Landsat TM and ASTER data. *Journal of Glaciology* **54** (187), 592–600. doi: 10.3189/002214308786570782.

Bolch T, Menounos B and Wheate R (2010*b*) Landsat-based inventory of glaciers in western Canada, 1985–2005. *Remote Sensing of Environment* **114** (1), 127–137. doi: 10.1016/j.rse.2009.08.015.

Bolch T, Pieczonka T and Benn DI (2011) Multi-decadal mass loss of glaciers in the Everest area (Nepal Himalaya) derived from stereo imagery. *Cryosphere* **5**(2), 349–358. doi: 10.5194/tc-5-349-2011.

Bookhagen B and Burbank DW (2006) Topography, relief, and TRMM-derived rainfall variations along the Himalaya. *Geophysical Research Letters* **33**(8). doi: 10.1029/2006GL026037.

Braithwaite RJ (2009) VK Raina and D Srivastava 2008. Glacier atlas of India. Bangalore, Geological Society of India. 315pp. ISBN-13: 978-8-185-86780-9. *Journal of Glaciology* **55**(193), 938–938.

Brun F, Wagnon P, Berthier E, Jomelli V, Maharjan SB, Shrestha F and Kraaijenbrink PDA (2019) Heterogeneous Influence of Glacier Morphology on the Mass Balance Variability in High Mountain Asia. *Journal of Geophysical Research: Earth Surface* **124**(6), 1331–1345. doi: 10.1029/2018JF004838.

Bush ABG and Bishop MP (2018) Glaciers, topography, and climate, *in*: Encyclopedia of the Anthropocene. *Elsevier* **2**, 71–79. doi: 10.1016/B978-0-12-809665-9.00158-0.

Chand P and Sharma MC (2015) Glacier changes in the Ravi basin, North-Western Himalaya (India) during the last four decades (1971–2010/13). *Global and Planetary Change* **135**, 133–147. doi: 10.1016/j.gloplacha.2015.10.013.

Chudley TR, Miles ES and Willis IC (2017) Glacier characteristics and retreat between 1991 and 2014 in the Ladakh range, Jammu and Kashmir. *Remote Sensing Letters* **8**(6), 518–527. doi: 10.1080/2150704X.2017.1295480.

Das S and Sharma MC (2018) Glacier changes between 1971 and 2016 in the Jankar Chhu Watershed, Lahaul Himalaya, India. *Journal of Glaciology* **65** (249), 13–28. doi: 10.1017/jog.2018.77.

DeBeer CM and Sharp MJ (2009) Topographic influences on recent changes of very small glaciers in the Monashee Mountains, British Columbia, Canada. *Journal of Glaciology* **55**(192), 691–700. doi: 10.3189/002214309789470851.

Dobhal DP, Mehta M and Srivastava D (2013) Influence of debris cover on terminus retreat and mass changes of Chorabari Glacier, Garhwal region, central Himalaya, India. *Journal of Glaciology* **59**(217), 961–971. doi: 10.3189/2013JoG12J180.

Frey H, Paul F and Strozzi T (2012) Compilation of a glacier inventory for the western Himalayas from satellite data: methods, challenges, and results. *Remote Sensing of Environment* **124**, 832–843. doi: 10.1016/j.rse.2012.06.020.

Garg PK, Shukla A and Jasrotia AS (2017) Influence of topography on glacier changes in the central Himalaya, India. *Global and Planetary Change* **155**, 196–212. doi: 10.1016/j.gloplacha.2017.07.007.

Granshaw FD and Fountain AG (2006) Glacier change (1958–1998) in the north Cascades national park complex, Washington, USA. *Journal of Glaciology* **52**(177), 251–256. doi: 10.3189/172756506781828782.

Hall DK, Bayr KJ, Schöner W, Bindschadler RA and Chien JY (2003) Consideration of the errors inherent in mapping historical glacier positions in Austria from the ground and space (1893–2001). *Remote Sensing of Environment* **86**(4), 566–577. doi: 10.1016/S0034-4257(03)00134-2.

Harris I, Osborn TJ, Jones P and Lister D (2020) Version 4 of the CRU TS monthly high-resolution gridded multivariate climate dataset. *Scientific Data* **7**(1), 1–18. doi: 10.6084/m9.figshare.11980500.

Hock R and 14 others (2019) High Mountain areas. In Pörtner H-O, Roberts DC, Masson-Delmotte V, Thai P, Tignor M, Poloczanska E, Mintenbeck K, Alegría A, Nicolai M, Okem A, Petzold J, Rama B and Weyer NM (eds), *IPCC Special Report on the Ocean and Cryosphere in a Changing Climate*. Cambridge, UK and New York: Cambridge University Press, pp. 131–202. doi: 10.1017/9781009157964.004

Hugonnet R and 10 others (2021) Accelerated global glacier mass loss in the early twenty-first century. *Nature* **592**, 726–731. doi: 10.1038/s41586-021-03436-z.

Huss M and Fischer M (2016) Sensitivity of very small glaciers in the Swiss Alps to future climate change. *Frontiers in Earth Science* **4**, 248. doi: 10.3389/feart.2016.00034.

Immerzeel WW and 30 others (2020) Importance and vulnerability of the world's water towers. *Nature* **577**(7790), 364–369. doi: 10.1038/s41586-019-1822-y.

King O, Bhattacharya A, Bhambri R and Bolch T (2019) Glacial lakes exacerbate Himalayan glacier mass loss. *Scientific Reports* **9**(1). doi: 10.1038/s41598-019-53733-x.

Kirkbride MP and Deline P (2013) The formation of supraglacial debris covers by primary dispersal from transverse englacial debris bands. *Earth Surface Processes and Landforms* **38**(15), 1779–1792. doi: 10.1002/esp.3416.

Koblet T and 6 others (2010) Reanalysis of multi-temporal aerial images of Storglaciären, Sweden (1959–99) – part 1: determination of length, area, and volume changes. *The Cryosphere* **4**, 333–343. doi: 10.5194/tc-4-333-2010.

Kraaijenbrink PDA, Bierkens MFP, Lutz AF and Immerzeel WW (2017) Impact of a global temperature rise of 1.5 degrees Celsius on Asia's glaciers. *Nature* **549**(7671), 257–260. doi: 10.1038/nature2387.

https://doi.org/10.1017/jog.2022.87 Published online by Cambridge University Press

Kulkarni AV, Bahuguna IM, Rathore BP, Singh SK, Randhawa SS, Sood RK and Dhar S (2007) Glacial retreat in Himalaya using Indian remote sensing satellite data. *Current Science*, **92**(1), 69–74.

Kulkarni AV and Karyakarte Y (2014) Observed changes in Himalayan glaciers. *Current Science* **106**(2), 237–244. doi: 10.18520/cs/v106/i2/237-244.

Kumar V, Mehta M, Mishra A and Trivedi A (2017) Temporal fluctuations and frontal area change of Bangni and Dunagiri glaciers from 1962 to 2013, Dhauliganga Basin, central Himalaya, India. *Geomorphology* **284**, 88–98. doi: 10.1016/j.geomorph.2016.12.012.

Laha S and 7 others (2017) Evaluating the contribution of avalanching to the mass balance of Himalayan glaciers. *Annals of Glaciology* **58**(75), 110–118. doi: 10.1017/aog.2017.27.

Mandal ST and Sharma MC (2020) Spatial changes in glaciers between 1965 and 2018 in Tirungkhad Watershed, Upper Sutlej Basin, Himachal Pradesh. *Earth Systems and Environment* **4**(2), 427–438. doi: 10.1007/s41748-020-00159-5.

Maurer JM, Schaefer J, Rupper S and Corley A (2019) Acceleration of ice loss across the Himalayas over the past 40 years. *Science Advances* **5**(6). doi: 10.1126/sciadv.aav7266.

Mehta M, Dobhal DP and Bisht MPS (2011) Change of Tipra glacier in the Garhwal Himalaya, India, between 1962 and 2008. *Progress in Physical Geography* **35**(6), 721–738. doi: 10.1177/0309133311411760.

Mir RA, Jain SK, Jain SK, Thayyen RJ and Saraf AK (2017) Assessment of recent glacier changes and its controlling factors from 1976 to 2011 in Baspa Basin, Western Himalaya. *Arctic, Antarctic, and Alpine Research* **49**(4), 621–647. doi: 10.1657/AAAR0015-070.

Mishra A, Nainwal HC, Dobhal DP and Shankar R (2021) Volume estimation of glaciers in Upper Alaknanda Basin, Garhwal Himalaya using numerical and scaling methods with limited field based data. *Himalayan Geology* **42**(2), 336–344.

Mishra A, Negi BDS, Banerjee A, Nainwal HC and Shankar R (2018) Estimation of ice thickness of the Satopanth Glacier, Central Himalaya using ground penetrating radar. *Current Science* **114**(4), 785–791. doi: 10.18520/cs/v114/i04/785-791.

Mukherjee K, Bhattacharya A, Pieczonka T, Ghosh S and Bolch T (2018) Glacier mass budget and climate reanalysis data indicate a climatic shift around 2000 in Lahaul-Spiti, western Himalaya. *Climatic Change* **148**(1), 219–233. doi: 10.1007/s10584-018-2185-3.

Nainwal HC and 6 others (2007) Chronology of the Late Quaternary glaciation around Badrinath (Upper Alaknanda basin): preliminary observations. *Current Science* **93**(1), 90–96.

Nainwal HC, Banerjee A, Shankar R, Semwal P and Sharma T (2016) Shrinkage of Satopanth and Bhagirath Kharak Glaciers, India, from 1936 to 2013. *Annals of Glaciology* **57**(71), 131–139. doi: 10.3189/2016aog71a015.

Nainwal HC, Negi BDS, Chaudhary M, Sajwan KS and Gaurav A (2008) Temporal changes in rate of recession: evidences from Satopanth and Bhagirath Kharak glaciers, Uttarakhand, using Total Station Survey. *Current Science* **94**(5), 653–660.

Oerlemans J and 10 others (1998) Modelling the response of glaciers to climate warming. *Climate Dynamics* **14**(4), 267–274. doi: 10.1007/s003820050222.

Oerlemans J (2005) Atmospheric science: extracting a climate signal from 169 glacier records. *Science* **308**(5722), 675–677. doi: 10.1126/science.1107046.

Pandey P and Venkataraman G (2013) Changes in the glaciers of Chandra-Bhaga basin, Himachal Himalaya, India, between 1980 and 2010 measured using remote sensing. *International Journal of Remote Sensing* **34**(15), 5584–5597. doi: 10.1080/01431161.2013.793464.

Patel LK, Sharma P, Fathima TN and Thamban M (2018) Geospatial observations of topographical control over the glacier retreat, Miyar basin, Western Himalaya, India. *Environmental Earth Sciences* **77**(5). doi: 10.1007/s12665-018-7379-5.

Paul F and 9 others (2009) Recommendations for the compilation of glacier inventory data from digital sources. *Annals of Glaciology* **50**(53), 119–126. doi: 10.3189/172756410790595778.

Paul F and 19 others (2013) On the accuracy of glacier outlines derived from remote-sensing data. *Annals of Glaciology* **54**(63), 171–182. doi: 10.3189/2013AoG63A296.

Paul F and 25 others (2015) The glaciers climate change initiative: methods for creating glacier area, elevation change and velocity products. *Remote Sensing of Environment* **162**, 408–426. doi: 10.1016/j.rse.2013.07.043.

Pratap B, Dobhal DP, Mehta M and Bhambri R (2015) Influence of debris cover and altitude on glacier surface melting: a case study on Dokriani Glacier, central Himalaya, India. *Annals of Glaciology* **56**(70), 9–16. doi: 10.3189/2015AoG70A971.

Pritchard HD (2019) Asia's shrinking glaciers protect large populations from drought stress. *Nature* **569**(7758), 649–654. doi: 10.1038/s41586-019-1240-1.

Rabatel A, Dedieu JP and Vincent C (2005) Using remote-sensing data to determine equilibrium-line altitude and mass-balance time series: validation on three French glaciers, 1994–2002. *Journal of Glaciology* **51**(175), 539–546. doi: 10.3189/172756505781829106.

Racoviteanu AE, Arnaud Y, Williams MW and Manley WF (2015) Spatial patterns in glacier characteristics and area changes from 1962 to 2006 in the Kanchenjunga–Sikkim area, eastern Himalaya. *The Cryosphere* **9**, 505–523. doi: 10.5194/tc-9-505-2015.

Racoviteanu AE, Paul F, Raup B, Khalsa SJS and Armstrong R (2009) Challenges and recommendations in mapping of glacier parameters from space: results of the 2008 global land ice measurements from space (GLIMS) workshop, Boulder, Colorado, USA. *Annals of Glaciology* **50**(53), 53–69. doi: 10.3189/172756410790595804.

Ragettli S, Bolch T and Pellicciotti F (2016) Heterogeneous glacier thinning patterns over the last 40 years in Langtang Himal, Nepal. *The Cryosphere* **10**, 2075–2097. doi: 10.5194/tc-10-2075-2016, 2016.

Raina VK and Srivastava D (2008) *Glaciers Atlas of India*, 1st Edn. Bangalore: Geological society of India.

Raj KBG, Rao VV, Kumar KV and Diwakar PG (2017) Alarming recession of glaciers in Bhilangna basin, Garhwal Himalaya, from 1965 to 2014 analysed from Corona and Cartosat data. *Geomatics, Natural Hazards and Risk* **8**(2), 1424–1439. doi: 10.1080/19475705.2017.1339736.

Rau F, Mauz F, Vogt S, Khalsa SJS and Raup B (2005) *Illustrated GLIMS Glacier Classification Manual Glacier, Classification Guidance for the GLIMS Glacier Inventory*. p. 36. Institut für Physische Geographie Freiburg, Germany, and National Snow and Ice Data Center, Boulder, USA. www.glims.org/MapsAndDocs/assets/GLIMS_Glacier-Classification-Manual_V1_2005-02-10.pdf [last access: 01/12/2022].

Remya SN, Kulkarni AV, Hassan ST and Nainwal HC (2020) Glacier mass loss in the Alaknanda basin, Garhwal Himalaya on a decadal scale. *Geocarto International* **37**(10), 3014–3032. doi: 10.1080/10106049.2020.1844309.

RGI Consortium (2017) *Randolph Glacier Inventory – A Dataset of Global Glacier Outlines: Version 6.0: Technical Report, Global Land Ice Measurements from Space*. Colorado, USA: Digital Media. Available at doi: 10.7265/N5-RGI-60.

Rounce DR, Hock R and Shean DE (2020) Glacier mass change in High Mountain Asia through 2100 using the open-source python glacier evolution model (PyGEM). *Frontiers in Earth Science* **7**, 1–20. doi: 10.3389/feart.2019.00331.

Sahu R and Gupta RD (2020) Glacier mapping and change analysis in Chandra basin, Western Himalaya, India during 1971–2016. *International Journal of Remote Sensing* **41**(18), 6914–6945. doi: 10.1080/01431161.2020.1752412.

Sakai A (2019) Brief communication: updated GAMDAM glacier inventory over high-mountain Asia. *The Cryosphere* **13**(7), 2043–2049. doi: 10.5194/tc-13-2043-2019.

Sakai A and Fujita K (2017) Contrasting glacier responses to recent climate change in high-mountain Asia. *Scientific Reports* **7**(1), 1–8. doi: 10.1038/s41598-017-14256-5.

Salerno F and 6 others (2017) Debris-covered glacier anomaly? Morphological factors controlling changes in the mass balance, surface area, terminus position, and snow line altitude of Himalayan glaciers. *Earth and Planetary Science Letters* **471**, 19–31. doi: 10.1016/j.epsl.2017.04.039.

Sangewar CV and Shukla SP (2009) *Inventory of the Himalayan Glaciers*. Kolkata: Geological Survey of India: Special Publication no 43, p. 588.

Sattar A, Goswami A, Kulkarni AV and Das P (2019) Glacier-surface velocity derived ice volume and retreat assessment in the Dhauliganga basin, central Himalaya – a remote sensing and modeling based approach. *Frontiers in Earth Science* **7**(105). doi: 10.3389/feart.2019.00105.

Scherler D, Bookhagen B and Strecker MR (2011) Spatially variable response of Himalayan glaciers to climate change affected by debris cover. *Nature Geoscience* **4**(3), 156–159. doi: 10.1038/ngeo1068.

Schmidt S and Nüsser M (2012) Changes of high altitude glaciers from 1969 to 2010 in the Trans-Himalayan Kang Yatze Massif, Ladakh, northwest

https://doi.org/10.1017/jog.2022.87 Published online by Cambridge University Press

India. *Arctic, Antarctic, and Alpine Research* **44**(1), 107–121. doi: 10.1657/1938-4246-44.1.107.

Shah SS, Banerjee A, Nainwal HC and Shankar R (2019) Estimation of the total sub-debris ablation from point-scale ablation data on a debris-covered glacier. *Journal of Glaciology* **65**(253), 759–769. doi: 10.1017/jog.2019.48.

Shean D (2017) *High Mountain Asia 8-Meter DEM Mosaics Derived from Optical Imagery, Version 1* [Online]. Boulder, CO: NASA National Snow and Ice Data Center Distributed Active Archive Center. Available at doi: 10.5067/KXOVQ9L172S.

Shrestha AB and Aryal R (2011) Climate change in Nepal and its impact on Himalayan glaciers. *Regional Environmental Change* **11**, S65–S77. doi: 10.1007/s10113-010-0174-9.

Shukla A and Garg PK (2020) Spatio-temporal trends in the surface ice velocities of the central Himalayan glaciers, India. *Global and Planetary Change* **190**(103187). doi: 10.1016/j.gloplacha.2020.103187.

Shukla A, Garg S, Mehta M, Kumar V and Shukla UK (2020) Temporal inventory of glaciers in the Suru sub-basin, western Himalaya: impacts of regional climate variability. *Earth System Science Data* **12**(2), 1245–1265. doi: 10.5194/essd-12-1245-2020.

Shukla A and Qadir J (2016) Differential response of glaciers with varying debris cover extent: evidence from changing glacier parameters. *International Journal of Remote Sensing* **37**(11), 2453–2479. doi: 10.1080/01431161.2016.1176272.

Singh O, Arya P and Chaudhary BS (2013) On rising temperature trends at Dehradun in Doon valley of Uttarakhand, India. *Journal of Earth System Science* **122**(3), 613–622.

Thakuri S and 6 others (2014) Tracing glacier changes since the 1960s on the south slope of Mt. Everest (central Southern Himalaya) using optical satellite imagery. *The Cryosphere* **8**(4), 1297–1315. doi: 10.5194/tc-8-1297-2014.

Thayyen R and Gergan J (2010) Role of glaciers in watershed hydrology: a preliminary study of a 'Himalayan catchment'. *The Cryosphere* **4**(1), 115–128. doi: 10.5194/tc-4-115-2010.

Valdiya KS, Paul SK, Chandra T, Bhakuni SS and Upadhyay RC (1999) Tectonic and lithological characterization of Himadri (Great Himalaya) between Kali and Yamuna rivers, Central Himalaya. *Himalayan Geology* **20**(2), 1–17.

https://doi.org/10.1017/jog.2022.87 Published online by Cambridge University Press